ADDIS ABABA UNIVERSITY
SCHOOL OF GRADUATE STUDIES
DEPARTMENT OF CHEMISTRY



Graduate project
(Chem-774)

Electrocatalytic Reduction of Oxygen at Poly(o-phenylenediamine) and Poly(3,4- ethylenedioxythiophene) at a Carbon Nanotube Modified Glassy Carbon Electrodes

By: Alemwork Abate

Advisor: Shimelis Admassie (PhD)

A Project Report Submitted to the School of Graduate Studies in Partial Fulfillment of the Requirements for the Degree of Master of Science in Chemistry

June, 2010

Addis Ababa University
School of Graduate Studies

Electrocatalytic Reduction of Oxygen at Poly(o-phenylenediamine) and Poly(3,4- ethylenedioxythiophene) at a Carbon Nanotube Modified Glassy Carbon Electrodes.

By

Alemwork Abate

Department of Chemistry

Approved by the examining board: Signature

Dr.Shimelis Admassie _____

(Advisor)

Prof. Theodros Solomon _____

(Examiner)

Dr. Ahmed Mustefa _____

(Examiner)

1. Acknowledgment

First of all I would like to praise the almighty God for his mercy upon me.

I am deeply indebted to my advisor, Dr. Shimelis Admassie, for his scholarly guidance, unreserved encouragement, and liberal provision of materials and meticulously correcting of this work.

My heartfelt thanks gose to Legesse Garedew, Tsion Ayalew, Belete Tesfaw and Asfaw Negash for their inspiring appreciation, provision of materials, and moral support in all of my study in the postgraduate program.

Table of Contents

Contents **Pages**

Acknowledgment.....i

List of figures iV

Abbreviations.....Vi

Abstract.....Vii

1. **Introduction**.....1

1.1 Reaction Pathways for Oxygen Reduction Reaction.....1

1.2 Mechanistic Aspects of Oxygen Reduction.....2

1.3 Kinetics of Oxygen Reduction Reaction.....5

1.4 Electrocatalysts for Oxygen Reduction.....7

1.4.1. Noble Metals Based Electrocatalysis.....7

1.4.2. Non-noble Based Electrocatalyst.....8

1.5 Oxygen Reduction Reaction in Fuel Cells.....9

2. **Carbon Nanotube**.....11

2.1. Introduction.....11

2.2 .Carbon Nanotube Structure and Defects.....11

2.3 Special Properties of Carbon Nanotubes.....12

2.4 Fictionalization of Carbon Nanotubes.....13

2.5 Electropolymerization of Carbon Nanotube.....14

2.6 Carbon Nanotubes-modified Electrodes for Oxygen ReductionReaction…….…..15

2.6.1. Carbon nanotubes–nanoparticles Composites.....15

2.6.2. Carbon Nanotubes-conducting Polymer Composites.....16

3. Electrochemical Kinetics, Techniques and Processes.....18

3.1. Electrode Process.....18

3. 2. Electrochemical Process.....18

3.2.1 Electrochemical Cell.....19

3.2.2. The Electrolyte Solution.....20

3. 3. Electrochemical Techniques.....20

3. 3.1 Cyclic Voltammetry.....20

3.3. 2 Rotating Disk Voltammetry 21

4. Experimental.....25
4.1. Objectives.....25
4. 2. Apparatus.....25
4.3. Chemicals and Reagents.....25
4.4. Preparation of the Modified Electrodes.....26
5. Results and Discussion.....27
5.1. Electrochemical Polymerization …….....27
5.1.1. Electrochemical Polymerization of oPDA.....27
5.1.2. Electrochemical Polymerization of EDOT.....28
5.2. Cyclic Voltammetric Investigation of the Electrocatalytic Reduction of Oxygen (CV).....30
5.2.1. Electrocatalytic Reduction of Oxygen at GC/MWCNT/PoPDA.....30
5.2.2. Electrocatalytic Reduction of Oxygen at GC/MWCNT/PEDOT.....31
5.3. Rotating Disk Voltammetric Investigation of the Electrocatalytic Reduction of Oxygen 32
5.3.1. Oxygen Reduction at MWCNT Modified Glassy Carbon Electrode.....32
5.3.2 Oxygen Reduction at MWCNT/PoPDA Modified Glassy Carbon Electrode 38
6. Conclusion 45
7. References 46

List of Figures

Figure 1. Molecular orbital diagram of oxygen molecule.....3

Figure 2. Possible configurations of oxygen interaction with a metal in a complex.....4

Figure 3. Schematic presentation of oxygen reduction reaction pathway suggested by Wroblowa.....5

Figure 4. Some of the important electrochemical devices 10

Figure 5. The chemical structure of common polymers used for electro grafting on to carbon nanotubes: 1) polyacrylonitrile, 2) polypyrrole,3) poly-N-(vinyl-carbazole),4) poly-(o-phenylenediamine) 5) polyaniline.....14

Figure 6. A complete cell stand: (a) cyclic voltammetry and (b) rotating disk voltammetry.....19

Figure 7. (a) potential-time exitation signal and (b) cyclic voltammogram for a reversible ($O + ne^- \rightleftharpoons R$) redox process.....21

Figure 8. Cyclic voltammogram for the electropolymeriztion of oPDA (○) at glassy carbon electrode (●) at multi-wall carbon nanotube modified glassy carbon electrode at a scan rate of 50 mV.....27

Figure 9.Cyclic voltammogram for the electropolymeriztion of EDOT(○) at GC and (●) at GC/MWCNT at a scan rate of 50 mV/s, in 0.1M tetrabutylammonium tetrafluoroborate in acetonitrle.....28

Figure 10. Cyclic voltammogram of monomer free PEDOT (□) at GC (●) at GC/MWCNT at a scan rate of 50 mV/s.....29

Figure 11. Cyclic voltammograms for the reduction of oxygen in oxygen saturated 0.2 M Na_2SO_4 (PH = 1.0) solution at (□) GC, (✳) GC/PoPDA, (●) GC/MWCNT, and (▲) GC/MWCNT/PoPDA at 20 mV/s.....30

Figure 12. Cyclic voltammograms for the reduction of oxygen in Ar saturated 0.2 M Na_2SO_4 at (□) GC/PEDOT, (▲) GC/MWCNT/PEDOT and in oxygen saturated 0.2M Na_2SO_4 (PH= 1.0) solution at (●) GC/PEDOT, (★) GC/MWCNT, (✳) GC/MWCNT/PEDOT at 20 mV/s.....31

Figure 13. Rotating disk voltammogram for the reduction of oxygen at GC/MWCNT rotating disk electrode at (○)100 rpm (Ar saturated) and (●) 100, (▼) 200, (✳) 400, (▲) 800 and (★) 1600 (rpm) in O_2 saturated 0.2M Na_2SO_4 at PH = 1.0, 10mV/s.....32

Figure 14. Levich plots for the reduction of oxygen at MWCNT modified glassy carbon electrode in (O_2 saturated 0.2M Na_2SO_4,10mV/s).....33

Figure 15. Koutecky- levich plot I_d^{-1} vs $\omega^{-1/2}$ for the reduction of oxygen at GC/MWCNT rotating disk electrode (O_2 saturated 0.2M Na_2SO_4, 10mV/s) for theoretical (2es and 4es) and experimental result.....34

Figure 16. Koutecky-levich plot I_d^{-1} vs $\omega^{-1/2}$ for the reduction of oxygen at GC/MWCNT rotating disk electrode (O_2 saturated 0.2M Na_2SO_4, 10mV/s) at different potentials.....35

Figure 17. Plot of $1/i_k$ vs the electrode potential for the reduction of oxygen at GC/MWCNT rotating disk electrode(O_2 saturated 0.2M Na_2SO_4,10mV/s).....36

Figure 18. Plot $\ln[i_k/ (i_l - i_k)]$ vs the electrode potential E for the reduction of oxygen at GC/MWCNT rotating disk electrode (O_2 saturated 0.2M Na_2SO_4, 10mV/s).....37

Figure 19. Rotating disk voltammogram for the reduction of oxygen at GC/MWCNT/PoPDA rotating disk electrode at (○)100 rpm (Ar saturated) and (●) 100, (★) 200, (▼) 400, (✳) 800 and (▲)1600 (rpm) inO_2 saturated 0.2M Na_2SO_4 at PH1.0, 10mV/s.....38

Figure 20. Levich for the reduction of oxygen at GC/MWCNT/PoPDA rotating disk electrode (O_2 saturated 0.2M Na_2SO_4, 10mV/s).....39

Figure 21. Koutecky-levich plot I_d^{-1} vs $\omega^{-1/2}$ for the reduction of oxygen at GC/MWCNT/PoPDA rotating disk electrode (O_2 saturated 0.2M Na_2SO_4, 10mV/s) for theoretical (2es and 4es) and experimental result.....40

Figure 22. Koutecky- levich plot I_d^{-1} vs $\omega^{-1/2}$ for the reduction of oxygen at GC/MWCNT/PoPDA rotating disk electrode (O_2 saturated 0.2M Na_2SO_4, 10mV/s) at different potentials.....41

Figure 23. Plot of $1/i_k$ vs the electrode potential for the reduction of oxygen at GC/MWCNT/PoPDA rotating disk electrode (O_2 saturated 0.2M Na_2SO_4,10mV).....42

Figure 24. Plot $\ln[i_k/ (i_l - i_k)]$ vs the electrode potential E for the reduction of oxygen on GC/MWCNT/PoPDA rotating disk electrode (O_2 saturated 0.2M Na_2SO_4, 10mV/s).....43

List of Abbreviations

ORR	Oxygen reduction reaction
PEMFC	Polymer exchange membrane fuel cell
DMFC	Direct-methanol fuel cell
AFC	Alkaline fuel cell
PAFC	Phosphoric-acid fuel cell
SOFC	Solid oxide fuel cell
MCFC	Molten-carbonate fuel cell
GCE	Glassy carbon electrode
PMEs	Polymer-modified electrodes
CNT	Carbon nanotube
SWCNT	singlewall carbon nanotube
MWCNT	Multiwall carbon nanotube
PoPDA	Poly(o-phenylenediamaine)
PEDOT	Poly (3,4-ethylenedioxy thiophene)
CV	Cyclic voltammetry
RDV	Rotating disk Voltammetry
RDE	Rotating disk electrode

Abstract

Electrochemical behaviour and electrocatalytic reduction of oxygen has been studied at PoPDA, and PEDOT mutiwall carbon nano-tube (MWCNT) composite film modified glassy carbon electrode. Cyclic and rotating disk voltammetric techniques were used to investigate the electrocatalytic activity of MWCNT composite film electrodes for oxygen reduction reaction (ORR). Glassy carbon electrodes modified with multiwall carbon nanotube by casting functionalized carbon nanotube was electropolymerized by using oPDA and EDOT. Koutecky-levich analysis at rotating disk electrode made possible to evaluate the kinetic parameters; total number of exchanged electron, limiting current, Tafel slope and exchange current density. Composites of PoPDA multi-wall carbon nanotube shows enhanced electrocatalytic activity for oxygen reduction reaction but the composite of PEDOT does not show electrocatalytic activity for oxygen reduction reaction.

Keywods: ORR, MWCNT, Electrocatalysis, Electropolymerization, Overpotential, Tafel slope, exchange current density.

1. Introduction

Oxygen (O_2) is the most abundant element in the Earth's crust. The oxygen reduction reaction (ORR) is also the most important reaction in life processes as in biological respiration, and in energy converting systems such as fuel cells. Normally the fuel cell developers concentrate on the anode electrode since this is involved in the combustion of the fuel and directly involved in the performance of the fuel cell. However, the counter cathode reaction is also equally important. Therefore developing suitable condition which can promote oxygen reduction reaction in an appropriate manner in terms of suitable electrode, reaction kinetics and also stability under the operating conditions and atmosphere are important factors that have been considered so far.[1] Normally, the ORR kinetics is very slow. In order to speed up the ORR kinetics to reach a practical usable level in a fuel cell, a cathode ORR catalyst was needed. At the current stage in technology, platinum (Pt)-based materials are the most practical catalysts. Because these Pt-based catalysts are too expensive for making commercially viable fuel cells, extensive research over the past several decades has focused on developing alternative catalysts. These ectrocatalysts include non noble metals and alloys, carbon materials, quinone and derivatives, transition metal macro cyclic compounds, transition metal chalcogenides, and transition metal carbides.[2-4]

1.1. Reaction Pathways for Oxygen Reduction Reaction

Oxygen reduction reaction (ORR) has been studied over the years because of its fundamental complexity, great sensitivity to the electrode surface, and sluggish kinetics. The sluggish kinetics of ORR under the conditions employed in electrochemical devices is due to the low partial pressure of oxygen in air, slow flow rate of oxygen (i.e., less residence time for oxygen molecules on active sites) under ambient conditions.[4]

ORR in aqueous solutions occurs mainly by two pathways: the direct 4-electron reduction pathway from O_2 to H_2O:

$$O_2 + 4\,H^+ + 4e^- \rightarrow 2\,H_2O \quad E^o = 1.229V \text{ Vs NHE (acidic media)} \qquad 1$$

$$O_2 + 2H_2O + 4e^- \rightarrow 4\,OH^- \quad E^o = 0.401V \text{ (alkaline media)} \qquad 2$$

The peroxide 2-electron reduction pathway from O_2 to H_2O_2:

$$O_2 + 2\,H^+ + 2e^- \rightarrow H_2O_2 \quad E^o = 0.67\ V \text{ Vs NHE (Acidic media)} \qquad 3$$

Peroxide can undergo further reduction or decomposition

$$H_2O_2 + 2H^+ + 2e^- \rightarrow 2\,H_2O \quad E^o = 1.77\ V \qquad 4$$

$$2\,H_2O_2 \rightarrow 2\,H_2O + O_2 \qquad 5$$

In alkaline media

$$O_2 + H_2O + 2e^- \rightarrow HO_2^- + OH^- \quad E^o = -0.065\ V \qquad 6$$

The reaction is followed by further two-electron reduction or by decomposition

$$HO_2^- + H_2O + 2e^- \rightarrow 3\,OH^- \quad E^o = 0.867\ V\ ,\ E^0 = -0.065 \qquad 7$$

$$2HO_2^- \rightarrow 2\,OH^- + O_2 \qquad 8$$

In non-aqueous aprotic solvents 1-electron reduction pathway from O_2 to superoxide (O_2^-) can also occur. The electronic and morphological properties of the electrode surface (such as electrode material, solution pH and on electrode potential) will determine the extent to which the mechanism proceeds through 1-, 2-, and 4-electron reduction pathways and have unique significance, depending on the applications. In fuel cell processes, the 4-electron direct pathway is highly preferred. The 2-electron reduction pathway is used in industry for H_2O_2 production. The 1-electron reduction pathway is of importance in the exploration of the ORR mechanism.[2] To obtain maximum energy capacity, it is highly desirable to reduce O_2 via the $4e^-$ pathway. Pt and its alloys are known to promote the 4e- ORR pathway.[4, 5]

1.2. Mechanistic Aspects of Oxygen Reduction

Even though oxygen reduction reaction (ORR) appears to be simple, it is quite complex. The molecular orbital diagram of oxygen molecule was shown in Figuer1. According to Hund's rule, in the ground-state, O_2 possesses two unpaired electrons located in a doubly degenerate π^* antibonding orbital. This corresponds to a triplet state. The bonding orbitals of oxygen molecule can be ascribed to the $3\sigma g$ orbital with two electrons, the doubly degenerate $1\pi u$

and 1πg * orbitals, where the 1πu orbital has double occupancy while the 1πg * orbital has single occupancy. The resulting bond order is two.

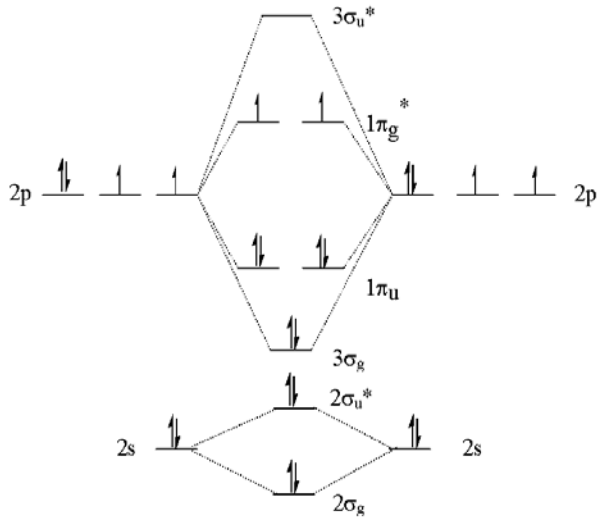


Figure 1. Molecular orbital diagram of oxygen molecule

When O_2 undergoes reduction, the electrons added occupy anti-bonding orbitals, decreasing the bond order of O-O. This increases the O-O bond distance and the vibrational frequency decreases. The excess of bonding over non-bonding electrons in the above diagram is four. This explains the high stability of the O_2 molecule and its relatively low reactivity, in spite of its high oxidizing power. The plausible 1:1 and 2:1 metal-dioxygen complex structures are given in Figure 2 Geometries 1 and 2 have been shown to give similar bonding patterns: each exhibits one σ and one π interaction.[5]

The Griffiths model (1), involves a side-on interaction of O_2 with the metal. The bonding can be viewed as arising from two contributions: σ type of bond formed by the overlap between mainly π orbital of oxygen and dz^2 orbital on the metal and a π back bond interaction between the metal d π orbitals and the partially occupied π* antibonding orbital on O_2.

In the Pauling model (2) which involves an end-on interaction of O_2 with the metal, a σ-bond is formed by the donation of electron density from the σ-rich orbital of dioxygen to an acceptor orbital dz^2 on the metal. The π interaction is produced between the metal d-orbitals (dxz, dyz) and π* orbital of dioxygen, with charge transfer from the metal to the O_2 molecule.

It indicates that the preference of geometries (1) and (2) is determined by the relative donating abilities of the filled π and σ orbitals of dioxygen molecule respectively.

Yeager (3) in 2:1 complexes of metal-dioxygen, the bonding arises from the interaction between the d-orbitals on the metal with π* and π orbitals combination on O_2 proposed the bridge interaction and it is likely to occur on noble metals such as Pt, face-to-face porphyrins where O_2 is reduced to water with little or no peroxide formed. A trans configuration is likely to occur on metal porphyrins, metal phthalocyanines, dimeric metal complexes.[6]



Griffiths model(1) Pauling model(2) Yeager(3)

Figure 2. Possible configurations of oxygen interaction with a metal in a complex.

Depending on the mode of adsorption of oxygen molecule on metal surface, different mechanistic steps will occur. Of various schemes proposed for ORR, a modified scheme proposed by Wroblowa et al. appears to be the appropriate one to describe the complicated reaction pathway for the reduction of O_2 at the metal surface (refer to Figure 3). At high potentials k_1/k_2 is constant with $k_1 > k_2$ indicating a direct reduction of oxygen to water than the two-electron reduction to peroxide. At intermediate potentials, k_1/k_2 ratio decreases indicating an increase in the two-electron reduction to peroxide. At lower potentials k_1/k_2 becomes lower than 1. However, k_3 increases resulting in a further reduction of peroxide to water before it escapes into solution. On most of the electrocatalysts, oxygen reduction takes place by the formation of high energy intermediate, H_2O_2 followed by further reduction to H_2O.

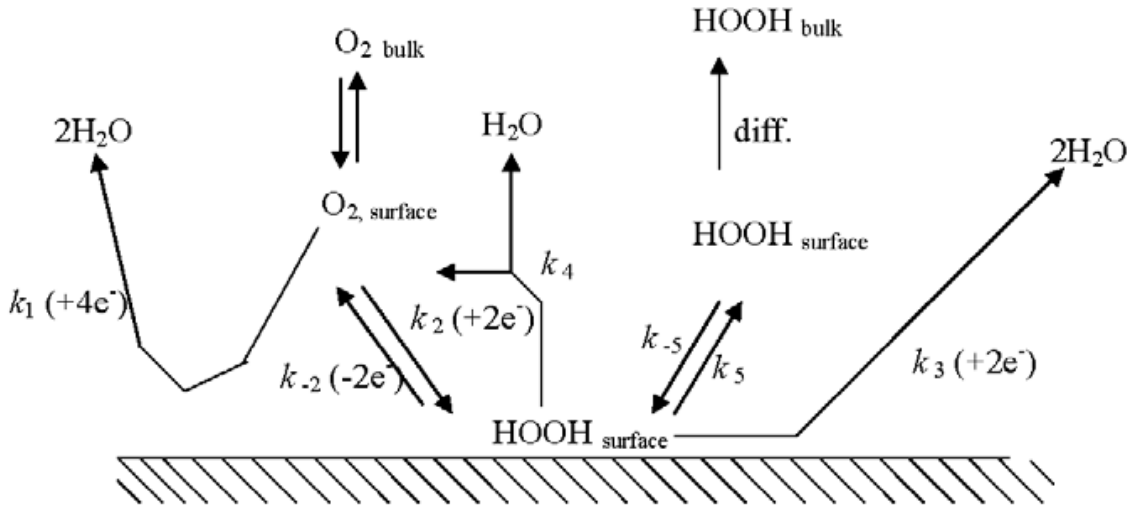


Figure 3. Schematic presentation of oxygen reduction reaction pathway suggested by Wroblowa

In order to obtain maximum efficiency and to avoid corrosion of carbon supports and other materials by peroxide, it is desired to achieve a four-electron reduction. The two electron reduction is of practical interest for the production of hydrogen peroxide. Finding suitable electro catalysts that can promote the direct four-electron reduction of oxygen molecule is an important task. [7]

1.3. Kinetics of Oxygen Reduction Reaction

It is desirable to have the O_2 reduction reaction occurring at potentials as close as possible to the reversible electrode potential (thermodynamic electrode potential) with a satisfactory reaction rate. The current-overpotential is given in Equation 9.

$$i_c = i^0{}_{O2}\left(\exp^{\frac{-n_{a0}a^0F\eta_c}{RT}} - \exp\frac{n_{a0}\left(1-a^0\right)F\eta_c}{RT}\right) \qquad 9$$

where i_c is the oxygen reduction reaction current density, i^0_{O2} is the exchange current density, n_{a0} is the number of electrons transferred in the rate determining step, $a0$ is the transfer coefficient, η is the overpotential of ORR, F is the Faraday constant, R is the gas constant, and T is the temperature in Kelvin. To obtain high current at low overpotential, the exchange current density i^o_{O2} should be large, and/or($RT/n_{a0}a^oF$) should be small.[8]

Tafel Slope

If the overpotential is large, the backward reaction is negligible and equation 9. can be simplified as

$$i_c = i^0 \exp\frac{n_{ao} a^0 F \eta_c}{RT} \qquad 10$$

The plot of η ~ log(i_c) gives a linear relationship, and the slope is 2.303RT/ $^{a0n}_{a0}$ ^{F} This slope is called the Tafel slope. Since all other parameters in the Tafel slope are known, the parameters determining the Tafel slope are actually ^{a0}and n_{a0}. The higher the Tafel slope, the faster the overpotential increases with the current density. Thus, for an electrochemical reaction to obtain a high current at low overpotential, the reaction should exhibit a low Tafel slope or a large $^{a0n}_{a0}$. For ORR, usually two Tafel slopes are obtained, 60 mV/dec and 120 mV/dec, respectively, depending on the electrode materials used and on the potential range. The electron transfer coefficient is a key factor determining the Tafel slope.

Exchange Current Density

Exchange current density is an important kinetic parameter representing the electrochemical reaction rate at equilibrium. For an electrochemical reaction, (O + ne- ↔ R) both forward and backward reactions can occur. At equilibrium, the net current density of the reaction is zero. The current density of the forward reaction equals that of the backward reaction. This current density is called exchange current density. The magnitude of the exchange current density determines how rapidly the electrochemical reaction can occur. The exchange current density of an electrochemical reaction depends on the reaction and on the electrode surface on which the electrochemical reaction occurs. For example, on a Pt electrode, the exchange current density of hydrogen oxidation is several orders larger than that of ORR. The O_2 reduction reaction shows a higher exchange current density on a Pt electrode than on an Au electrode. Therefore, electrode materials or catalysts have a strong effect on ORR kinetics. Different materials can give different exchange current densities. The exchange current density is related to the true electrode area and to the reactant concentration (or partial pressure, for a gas), especially for ORR on the Pt electrode in fuel cells. [10]

1.4. Electrocatalysts for Oxygen Reduction

Both noble and non-noble metal-based electrocatalysts were investigated for oxygen reduction. In the case of noble metal electrocatalysts, platinum-based materials appear to be the best, whereas in the case of non-noble metal electrocatalysts several materials were investigated depending on the temperature of operation of electrochemical devices. Transition metal chalcogenides and pyrolyzed macrocyclic compounds are two of the most widely studied non-noble metal catalysts for oxygen reduction in electrochemical devices operated at low temperatures whereas transition metal oxides are employed in ectrochemical devices operated at both low and high temperatures. Oxygen reduction takes place at high positive potentials. At such potentials most of the metals will dissolve and give rise to a similar situation to that prevailing at the cathode i.e., only noble metals and some of their alloys offer possibilities among metallic systems.[11]

1.4.1. Noble Metals Based Electrocatalysis

The most familiar oxygen reduction catalysts are based on noble metals, particularly platinum. These have been investigated extensively as pure metals, as nanoparticles and alloys, and as polycrystalline and single crystal surfaces. To date, conventional carbon supported platinum based materials are the most active, efficient, applicable and successful catalysts for electrochemical devices at the current technology stage. However, the problem associated with these Pt catalysts is the slowness of ORR, which is due to the formation of OH^- species at +0.8 V, which inhibits further reduction of oxygen and hence results in loss of performance. In order to compensate the loss of activity, one requires higher amounts of catalyst which dramatically increases the cost. However, there are several drawbacks to use Pt catalysts in fuel cells, beside the cost issue. Some of these are:[11]

(1) Pt catalyzed oxygen reduction is not a complete four-electron reaction.

(2) Pt catalysts are sensitive to contaminants.

(3) Methanol contamination of the cathode catalyst.

So researchers focused on alloys that prevents the adsorption of OH species, reduce oxygen selectively to water without being affected by the contaminants and tolerant to methanol. Among the alloys, Pt-Cr, Pt-Co and Pt- Fe show higher activity for ORR and tolerance for methanol.[12]

1.4.2. Non-noble Based Electrocatalysts

Transition metal oxides: Transition metal oxides, precisely because of their ability to switch between different valencies, possess appreciable chemical and/or electrocatalytic activity, which make them versatile materials for chemical and electrochemical reactions. For the same reasons, these oxides exhibit remarkable stability toward chemical and electrochemical attack in appropriate conditions. In general, transition oxides are of two types:

1) A porous, metallic oxide or a metallic oxide dispersed on or with carbon to form a porous metallic matrix. The oxide is catalytically active for the ORR (in the case of all electrochemical devices e.g., AFC, PAFC, PEMFC, DMFC, SOFC, MCFC, metal-air batteries and chlor-alkali cells). In this case, ORR occurs at a catalyst/electrolyte/air three phase linear interface.
2) A mixed electron/oxide-ion conductor that catalyzes the ORR is coated as a film on a solid oxide-ion electrolyte (in the case of SOFC and MCFC).

Transition metal chalcogenides: Chevrel phases based on metal clusters constitute another class of materials that show activity for oxygen reduction. Some of these materials selectively reduce oxygen to water even in the presence of methanol by the direct transfer of four electrons under acidic conditions, which makes them as promising cathode materials for electrochemical devices such as PEMFC and DMFC. Ternary chalcogenides of the formula $MxMo_6X_8$ (M= Cu, Ag, Ni, Fe, Pb, rare earth, etc. and X = S, Se, or Te) have been first synthesized by Chevrel et al. in 1971 and therefore are often referred to as Chevrel compounds.

Transition metal macrocycles: Macrocyclic derivatives of transition metals constitute a unique class of electro catalyst for oxygen reduction. One of the characteristics of an oxygen electrode is that it chemisorbs oxygen without degradation of the catalytically active surface. Reversible adsorption has been observed in aqueous solution for some metal chelates e.g., bis(salisylal) ethylene diamine cobalt(II), heme, and Co(II) histidine. The possible application of these soluble compounds as fuel cell (for cathode) catalysts would lead to a complicated engineering system, even if the oxygen exchange kinetics was favourable. A number of insoluble metal chelates will also chemisorb oxygen; the most chemically stable of these are metal porphyrins, metal phthalocyanines and metal tetraazannulenes to some extent. The

reason for exploiting these materials as oxygen reduction catalysts is due to their analogous structures of enzyme catalase, which decomposes oxygen in living cells.[13-15]

Other electrocatalysts: Owing to the good electrical conductivity, corrosion resistance and eventual catalytic activity, metal phosphides, metal nitrides, metal arsenides, metal tellurides and metal carbides were exploited for oxygen reduction in aqueous solutions. Mazza and Trasatti investigated the oxygen reduction activity of TiN, TiC, TaC and WC in acidic solutions. They observed superior activity of WC than other investigated systems. The order of activity is, TaC<TiC<TiN<WC. Later Giner and Swette evaluated the oxygen reduction activity of TiC and TiN in alkaline solutions and observed higher activity of TiN than TiC followed by Ti.

1.5. Oxygen Reduction Reaction in Fuel Cells

A fuel cell is an electrochemical device that converts hydrogen and oxygen into electricity without combustion. A fuel cell operates much like a battery, turning oxygen and hydrogen into electricity in the presence of an electrically conductive material called an electrolyte. But unlike a battery, it never loses its charge and will generate electricity as long as there is a source of hydrogen and oxygen.[16]

The fuel cells, however, provide comparable power to batteries and generate electricity continuously because of the continuous active materials (fuel) supply. The fuel cells produce moderate power but high energy. The fuel cell systems are simple and few. The product of the cell is generally water, which makes them “zero emission”. These advantages cause the fuel cell one of the most promising candidates for energy conversion. The electrochemical reduction of molecular oxygen is important especially for devices such as metal air batteries (e.g Zinc–air battery) and fuel cells. Therefore, the development of efficient catalysts and electrodes requires great focuses in order to improve the inefficiency specially in fuel cells. Oxygen reduction reaction is an important reaction, because it is the greatest sources of inefficiency in fuel cells. [3, 16]

Types of Fuel Cells [17-19]

There are different types of fuel cells, each using a different chemistry. Based on the operating temperature and the type of electrolyte used fuel cells are usually classified as

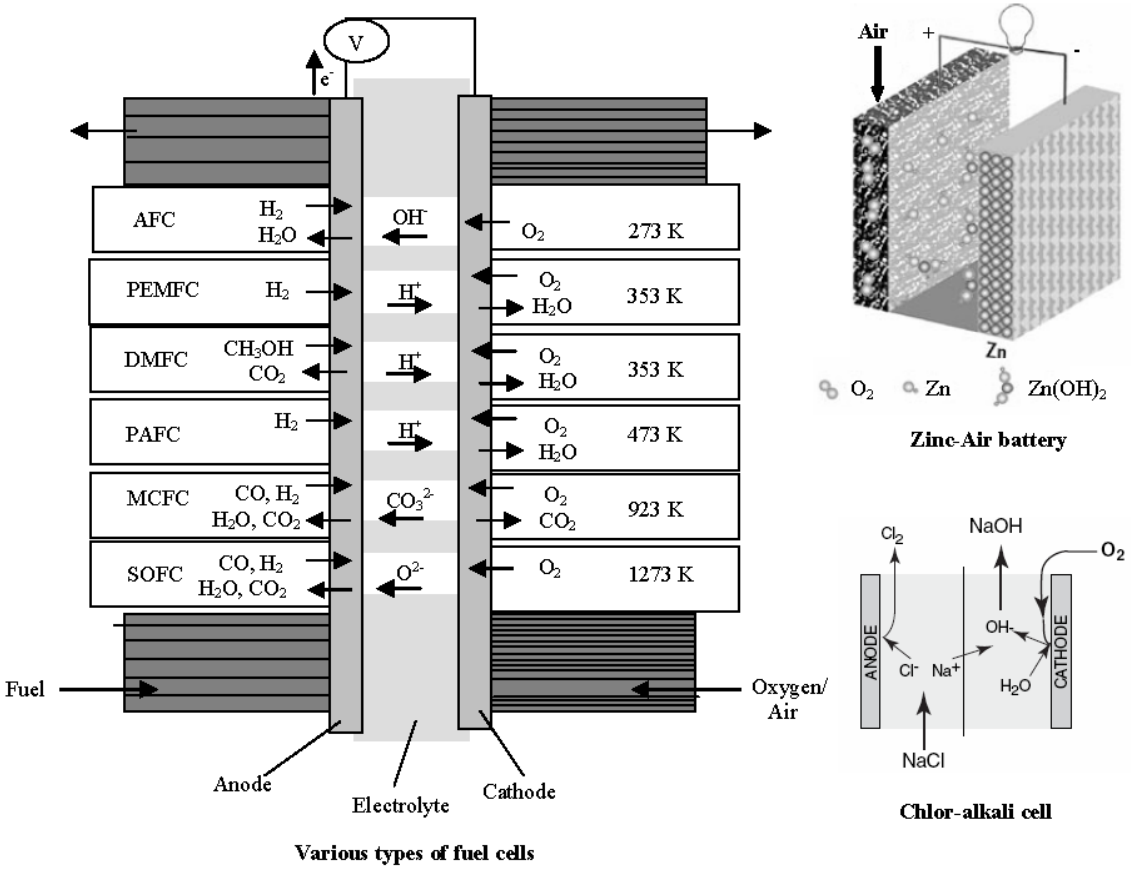


Figure 4. Some of the important electrochemical devices

- Polymer exchange membrane fuel cell (PEMFC)
- Direct-methanol fuel cell (DMFC)
- Alkaline fuel cell (AFC)
- Phosphoric-acid fuel cell (PAFC)
- Solid oxide fuel cell (SOFC)
- Molten-carbonate fuel cell (MCFC)

2. Carbon Nanotube

2.1 Introduction

Carbon nanotubes (CNTs) are allotropes of carbon with a cylindrical nanostructure. These cylindrical carbon molecules have novel properties that make them potentially useful in many applications; in nanotechnology, electronics, optics and other fields of materials science, as well as potential uses in architectural fields. They exhibit extraordinary strength and unique electrical properties, and are efficient thermal conductors. Nanotubes are members of the fullerene structural family, which also includes the spherical buckballs. Fullerenes are large, closed-cage, carbon clusters and have several special properties that were not found in any other compound before. The ends of a nanotube might be capped with a hemisphere of the buckyball structure. Their name is derived from their size, since the diameter of a nanotube is on the order of a few nanometers (approximately 1/50,000th of the width of a human hair), while they can be up to several millimeters in length). Nanotubes are categorized as single-walled carbon nanotubes (SWCNTs) and multi-walled carbon nanotubes (MWCNTs).[20] Carbon nanotubes are generally produced by three main techniques, arc discharge, laser ablation and chemical vapour deposition.

2.2. Carbon Nanotube Structure and Defects

Many exotic structures of fullerenes exist regular spheres, cones, tubes and more complicated and strange shapes. Here we will describe some of the most important and best-known structures. Single Walled CarbonNanotubes (SWCNT) can be considered as long wrapped graphene sheets. As stated before, nanotubes generally have a length to diameter ratio of about 1000 so they can be considered as nearly one-dimensional structures. More detailed, a SWCNT consists of two separate regions with different physical and chemical properties. The first is the sidewall of the tube and the second is the end cap of the tube. Multi Walled Carbon Nanotubes (MWCNT) can be considered as a collection of concentric SWCNTs with different diameters. The length and diameter of these structures differ a lot from those of SWCNTs and, of course, their properties are also very different. Introduction of defects can also result in various new structures such as Y-branches T-branches or SWCNT junctions. Under certain circumstances, these defects can be introduced in a ‘controlled’ way. These

defects result in special structures that will have other, but even more interesting, properties than their original forms. A final type of interesting structures is the so-called peapods, carbon nanotubes with C_{60} molecules enclosed in the nanotube.

The distance between two graphite sheets in MWCNT is typically 0.340 nm, slightly greater than the distance between two consecutive sheets in single crystal graphite, 0.335 nm, which may be explained by specific cylindrical geometry. CNT can be metallic or semiconducting, depending on the crystal structure of the graphene sheets. The electronic transport occurs ballistically (i.e. almost without scattering) in metallic nanotubes. This allows the nanotubes to conduct electricity with minimal resistance, thus diminishing heating. [20]

2.3. Special Properties of Carbon Nanotubes [20,21]

Electronic, molecular and structural properties of carbon nanotubes are determined to a large extent by their nearly one-dimensional structure. The most important properties of CNTs and their molecular background are stated below.

Chemical reactivity: The chemical reactivity of a CNT is compared with a graphene sheet. Carbon nanotube reactivity is directly related to the pi-orbital mismatch caused by an increased curvature. Therefore, a distinction must be made between the sidewall and the end caps of a nanotube. For the same reason, a smaller nanotube diameter results in increased reactivity. Covalent chemical modification of either sidewalls or end caps has shown to be possible. For example, the solubility of CNTs in different solvents can be controlled this way. Though, direct investigation of chemical modifications on nanotube behaviour is difficult as the crude nanotube samples are still not pure enough. The sites of highest chemical reactivity within carbon nanotubes are the caps, which have a fullerene-like structure.

Electrical conductivity: Depending on their chiral vector, carbon nanotubes with a small diameter is either semi-conducting or metallic. The differences in conducting properties are caused by the molecular structure that results in a different band structure and thus a different band gap.

Optical activity: Theoretical studies have revealed that the optical activity of chiral nanotubes disappears if the nanotubes become larger. Therefore, it is expected that other physical properties are influenced by these parameters too. Use of the optical activity might result in optical devices in which CNTs play an important role.

Mechanical strength: Carbon nanotubes have a very large Young modulus in their axial direction. The nanotube as a whole is very flexible because of the great length. Therefore, these compounds are potentially suitable for applications in composite materials that need anisotropic properties.

2.4. Functionalization of Carbon Nanotubes [21]

The carbon nanotube unique properties make it desirable for different applications. For most of these applications, nanotubes require functionalization, such as changing some of the graphite properties to make nanotubes soluble in different media, or attaching different groups even inorganic particles for future utilization of modified nanotubes. All functionalization methods of carbon nanotubes can be divided into two major groups

1. Functionalization from inside (endohedral), meaning that nanotubes are functionalized by filling them with different nanoparticles, this can be achieved either by
i) Exploiting the phenomenon of spontaneous penetration when nanotubes are filled with colloidal suspensions followed by evaporation of the carrier liquid
ii) Wet chemistry, when the nanotubes are filled with some compounds, which react under particular thermal or chemical conditions and produce nanoparticles. These nanoparticles then become trapped in the nanotubes.

2. Chemical functionalization from outside (exohedral).This group also can be subdivided into three subgroups based on the mechanism of attachment of different groups or compounds to the sidewall of the nanotube:
i) Covalent functionalization by attaching functional groups to the nanotube ends or defects
ii) Covalent functionalization through “sidewall functionalization”
iii) Noncovalent exohedral functionalization, for example, wrapping nanotubes by polymers

2.5. Electropolymerization of Carbon Nanotube [22]

There are ranges of publications dealing with the electropolymerization of appropriate monomers onto CNT thin film or bucky-paper electrodes. The most relevant polymers that have been used to coat CNTs in this manner are depicted in figure 5. In the initial stage, motivated by the wealth of data available on the corresponding conducting polymers, the experiments were focused on the electropolymerization of aniline and pyrrole. More recently,

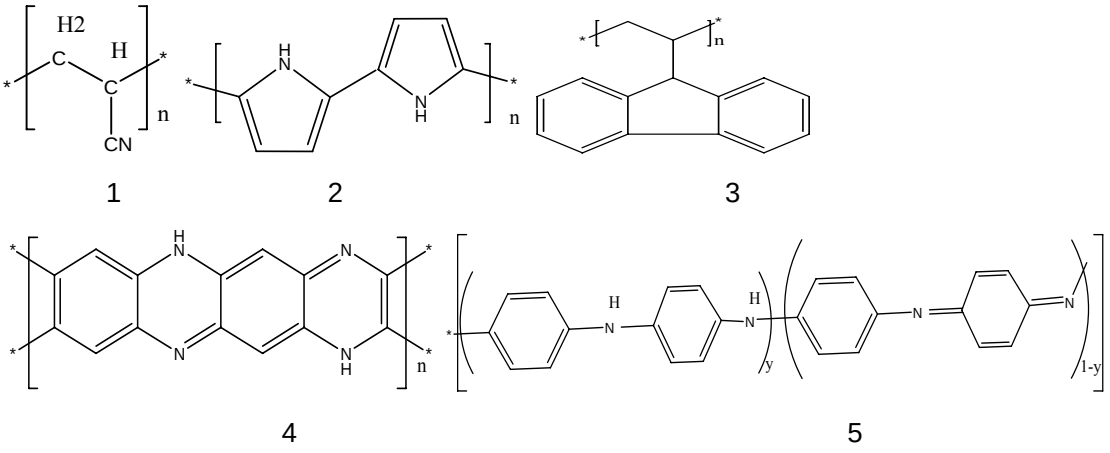


Figure 5.The chemical structure of common polymers used for electrografting onto carbon nanotubes:1) polyacrylonitrile, 2) polypyrrole, 3) poly-N-(vinyl-carbazole), 4) poly-(o-phenylenediamine) 5) polyaniline

polymer coatings obtained via electropolymerization of o-phenylenediamine onto oxidatively treated MWCNTs were found to strongly interact with the nanotubes via oxygen containing functional groups (presumably –COOH).This interaction has been interpreted as the origin of the enhanced polymer deposition rate in comparison to a bare glassy carbon electrode (GCE). It has been speculated that the created cationic radicals preferentially attach to the acidic sites on the nanotubes, thereby greatly increasing the number of nucleation sites for the polymerization reaction. This behaviour is different from that of polypyrrole, for which no facilitated grafting has been observed. Apart from polyaniline and polypyrrole, the electrodeposition of a few other polymers has been performed

2.6. Carbon Nanotubes Modified Electrodes for Oxygen Reduction Reaction [2, 20 and 23]

Modification is most usually carried out by coating or preparing CNTs-binder composite electrodes. Simple modified electrodes designs can be obtained by incorporation of a small volume of a CNTs dispersion onto a glassy carbon electrode. Methods for the preparation of homogeneous dispersions of CNTs, suitable for processing into thin films can be found in the review by Merkoc¸ i et al[20]. Simple modified electrodes designs can be obtained by

- Incorporation of a small volume of CNTs dispersion onto a glassy carbon electrode.
- Heating the GC and further abrasive immobilization of MWCNTs rubbing the electrode surface on a filter paper supporting the CNTs.

2.6.1. Carbon Nanotubes–nanoparticles Composites

Noble metals such as platinum [19], gold [24], ruthenium [26] and mixed metals [27] have played a dominating role as electrocatalysts for the ORR. However, the high cost of these metals restricts the commercial utility as catalyst. A search for low-cost electrocatalysts for the ORR has then been an important goal for many researchers. Recently, carbon nanotubes (CNTs) have attracted much interest from fundamental and applied perspectives owing to their good mechanical and unique electrical properties [28]. CNTs have been proved to be the suitable materials as electrodes or electrocatalyst supports due to their high electronic conductivity for the promotion of electron transfer reactions and better electrochemical and chemical stabilities in aqueous and non-aqueous solutions. CNT due to its high surface area and hollow geometry combined with its high electronic conductivity and use full mechanical property have the ability to promote electron transfer reaction when used as electrode material in electrochemical reaction. Recently, oxygen reduction reaction catalyzed by carbon nanotubes has been investigated by several groups [29,30], which found that the catalyzed ORR was dependent on the preparation method for the carbon nanotube films. [29]

The attractive physical and chemical properties of metal and metal-oxide nanoparticles have been widely exploited in the last years for electrochemical sensing applications. Incorporation of nanoparticles to CNTs electrode matrices has demonstrated to enhance the electrocatalytic efficiency of many electrochemical processes giving rise to several significant applications. Compton and co-workers have recently reviewed the methods for the preparation of CNT supported metal nano particle and further application. Different metal nano particle (Pt, Cu, Pd, Au, Co-porphyrin composite) can be attached to the surface of carbon nanotube and these hybrid electrodes demonstrate a high electrocatalitc activity towards various biochemical reaction. Recent studies showed that Polythionine/gold nanoparticles/multi-wall carbon nanotubes,[24] a novel nano-silver coated MWCNT composite, Gold, silver and palladium metal nanoparticles [28] MWCNT composite possess several catalytic effect on different reaction and in many case a fast electron transfer reaction rate is observed. The electrocatalytic reduction of molecular oxygen were studied at metal, metal nanoparticle or metal sited ligands due to electrocatalytic reduction of oxygen at reduced over potential but it was not cost effective. Thus, numerous efforts have been paid to search cheaper material to replace the costly Pt based electrocatalists. Gold nanoparticle (AuNp)/poly (diallyldimethylammonium chloride) multi wall carbon nanotube composite were also studied and it showed higher electro catalytic activity for oxygen reduction reaction.[31] It was also reported that modification of MWCNT with anthraquinone-1-diazonium chloride produces electro-catalytically active mediator sites for the reduction of oxygen[32]. A novel composite film, f-MWCNTs–NF–PtAu, made of functionalized multiwall carbon nanotubes (f-MWCNTs) with NF, nano Pt, and nano Au was also shows enhanced catalytic activity towards biochemical compounds.

2.6.2. Carbon Nanotubes-conducting Polymer Composites

Conducting polymer-modified electrodes have been one of the most preferred approaches for the preparation of electrochemical sensors since many years. The combination of the well known characteristics of conducting polymers (good stability, reproducibility, high number of active sites, strong adherence and homogeneity in electrochemical deposition) with those of CNTs leads to an improved performance of the resulting sensing devices, because of their complementary electrical, electrochemical and mechanical properties, and also to the synergic effect. Composites of conducting polymers and CNTs like polyaniline, polypyrrole,

and poly(p-phenylenevinylene) have been synthesised by either chemical or electrochemical polymerisation in the presence of CNTs. Regarding the chemical approach, an oxidant is needed and converted to a reducing product that may, if present, affect the properties of the product. Electrochemical polymerisation has a number of well-known advantages because the electrochemical variables can be adjusted to control the film thickness and other characteristics of the polymer coating. [33]

The ORR at electronically conducting polymers such as polyaniline (PANI), polypyrrole, Polythiophene, Poly(3-methylthiophene) and poly(3,4-ethylenedioxy thiophene) (PEDOT)-modified electrodes were studied .Glassy carbon modified with these polymers in oxygen-saturated electrolytes indicated electro catalytic activity towards the ORR with the exception of PEDOT. [34] An electronically conducting polymer film serves as a conductive matrix for the electron transfer reaction. Also, the introduction of the conducting polymer to electrocatalysts helps in increasing the interfacial properties between the electrode and electrolyte. Composite materials based on the combination of a conducting polymer and CNT have shown properties of the individual components with synergistic effect. The ability of CNT electrodes to promote the electron-transfer reactions of important molecules such as cytochrome [35], NADH [36], norepinephrine [37], hydrogen peroxide [38], hydrazine [39] has been well documented. Dispersion of catalyst material in a convenient electron conducting substrate is known to enhance the catalytic activity of the electrode [40, 41]. Preparation of modified electrode in which conducting polymer is present as connected unit to CNT and their catalytic activity towards ORR has been reported. For example glassy carbon electrode modified with polyaniline grafted multiwall carbon nanotube film has been enhanced electrocatalytic for dioxygen reduction.[32] It was also reported that in the electrocatalysis of MWCNTs, modified on a edge plane pyrolytic graphite (EPPG) electrode, both the reduction and oxidation currents were increased significantly compared to the results obtained on a bare EPPG electrode.[42] Polypyrrole-modified electrodes incorporating CNTs have been employed to construct enhanced enzyme electrochemical biosensors.

3. Electrochemical Kinetics, Techniques and Processes

3.1. Electrode Process

Electrode process involves all the changes and processes occurring at the electrode. Electrode processes consist of the rate of electron transfer and the mass transport controlled process. The mass transport occur by three different modes

- Diffusion- the spontaneous movement under the influence of concentration gradient (i.e., from regions of high concentration to regions of lower concentration), aimed at minimizing concentration differences.
- Convection-transport to the electrode by a gross physical movement; such fluid flow occurs with stirring or flow of the solution and with rotation or vibration of the electrode (i.e., forced convection) or due to density gradients (i.e., natural convection);
- Migration-movement of charged particles along an electric field (i.e., the charge is carried through the solution by ions according to their transference number).

Reaction controlled by rate of electron transferred; reactions are heterogeneous and take place in the interfacial region between electrode and solution, the region where charge distribution differs from that of the bulk phases. The electrode process is affected by the structure of this region. The electrode can act as only a source (for reduction) or a sink (for oxidation) of electrons transferred to or from species in solution, as in ($O + ne^- \rightarrow R$) where O and R are the oxidized and reduced species, respectively. Alternatively, it can take part in the electrode reaction, as in dissolution of a metal M ($M \rightarrow M^{+n} + ne^-$). In order for electron transfer to occur, there must be a correspondence between the energies of the electron orbital's (where transfer takes place in the donor and acceptor).[43]

3.2. Electrochemical Process

The success of an electrolysis process depends on the choice of a suitable electrochemical cell and optimal operation conditions because there is a widespread variety of electrolyte composition, cell constructions, electrode materials, and electrochemical reaction parameters.

3.2.1 Electrochemical Cell

Three-electrode cells are commonly used in controlled – potential experiments. Three electrodes are usually employed: a working, reference and counter (Auxiliary) electrodes.

Working electrodes: It is the electrode at which the reaction of interest occurs. The performance of the voltammetric procedure is strongly influenced by the working electrode material. A wide range of solid materials are used as electrodes. The most common 'inert' solid electrodes are lead, carbon (glassy carbon), gold and platinum. Glassy carbon has been very popular because of its excellent mechanical and electrical properties, wide potential window, chemical inertness (solvent resistance) and relatively reproducible performance. Electrode pretreatment are always needed in order to get reproducible data on solid electrodes. They are mostly focused on the removal of surface impurities (oxides). Electrodes can be polished with alumina of fixed grain size down to 0.05μm.



(a)



(b)

Figure 6. A complete cell stand: (a) cyclicvoltammetry and (b) rotating disk voltammetry.

Counter electrode: The purpose of the counter electrode is to supply the current required by the working electrode with out in any way limiting the measurement response of the cell. It is the current carrying electrode and must be inert and larger in dimension. Platinum wire or foil is the most common counter electrode.

Reference electrode: is an electrode which has a stable and well-known electrode potential. The role of the reference electrode is to provide a fixed potential which does not vary during the experiment. Some of the reference electrodes are Ag/AgCl, sat KCl, Hg/Hg_2Cl_2, sat KCl, Hg/Hg_2Cl_2 $moldm^{-3}$ KCl e.tc.[44]

3.2.2. The Electrolyte Solution

The electrolyte solution is the medium between the electrodes in the cell, and it will consist of solvent and a high concentration of an ionized salt (supporting electrolyte) as well as the electro active species.

The supporting electrolyte is present to increase the conductivity of the solution and hence to reduce the resistance between the working and the counter electrode and to effectively eliminate migration as a mode of mass transport for electroactive species.

Oxygen Removal

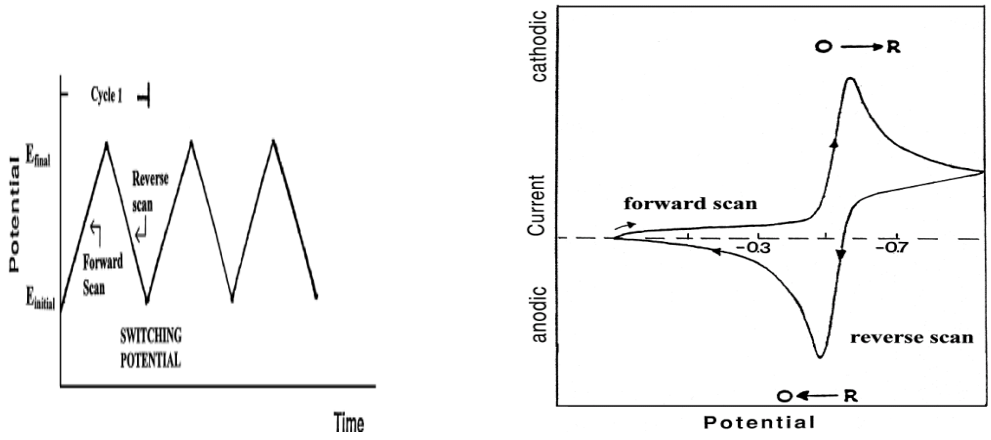
A variety of method can be used for the removal of dissolved oxygen. The most common method has been purging with an inert gas (usually purified nitrogen or Ar) for 15-20 minutes prior to recording of the voltammogram.

3.3. Electrochemical Techniques

3.3.1 Cyclic Voltammetry

Cyclic voltammetry (CV) is the most useful technique in electrochemistry. It can quickly provide qualitative information about catalysts and electrochemical reactions, such as the electrochemical response of catalysts and the catalytic activity of the catalysts with respect to some electrochemical reactions. The effectiveness of CV results from its capability for rapidly observing redox behavior over a wide potential range. The resulting voltammogram is analogous to a conventional spectrum in that it conveys information as a function of energy scan. CV consists of scanning linearly the potential of a stationary working electrode (in an

unstirred solution), using a triangular potential wave form. Depending on the information sought single or multiple cycle can be used. During the potential sweep, the potentiostate measures the current resulting from the applied potential. The cyclic voltammogram is a complicated, time dependent function of a large number of physical and chemical parameter. CV offers a rapid location of redox potentials of the electro active species (ORR) and a convenient evaluation of the effect of media on redox process.



a b

Figure 7.(a).Potential-time excitation signal and (b) Cyclic voltammogram for a reversible O + ne^- ⇌ R redox process

A cyclic voltammogram (Figure 7) can quickly show the presence of all the species that undergo redox reaction at the electrode within the limit set by the solvent, electrolyte and the electrode [44]

3.3. 2 Rotating Disk Voltammetry

Rotating disk electrode technique has become one of the most extensively used techniques for investigating the mechanism and kinetics parameters of a variety of electrochemical reaction. Its major advantage over other methods lies in its ability to separate, through suitable mathematical apparatus, the diffusion component of the current from its kinetic part. So that the analysis of each separate component can be made, leading to the determination of some overall kinetic parameters (number of electron transferred, slope, exchange and limiting current density). [45]

Rotating disk voltammetry (RDV) provides much more quantitative information because electrolysis occurs under forced convection. The electrochemical behavior of a mixed diffusion -kinetic system, such as the rotating disk electrode in aqueous electrolyte with negligible ionic resistance can be

$$\frac{1}{i_{obs}} = \frac{1}{i_l} + \frac{1}{i_k} \qquad 11$$

Where i_{obs} is experimentally observed current, i_k is current associated with the electrochemical kinetics and i_l the mass transport limiting current. Since i_k is the electrochemical kinetic current, all of the potential dependence lies in the i_k term. On the other hand, i_l, the mass transport limiting current, contains physical properties of the solution including V kinematics viscosity, and D the diffusion coefficient, C the concentration of oxygen in the solution and ω the electrode rotation rate.

In this technique, the electrode is rotated at an angular velocity of ω and the mass transfer limited current (i_L) depends only on the angular rotation velocity according to the following equation:

$$i_l = 0.62\, n\, F A\, D^{2/3}\, C\, \nu^{-1/6}\, \omega^{1/2} \qquad 12$$

Here n is the number of electron transferred, F is faraday constant, A is electrode area, ν is kinematics viscosity , and D is the diffusion coefficient , C the concentration of oxygen in the solution and ω the electrode rotation rate. A linear plot of i_L Vs $\omega^{1/2}$ implies that the electrocatalytic reaction is faster than the rate of substrate delivered to the electrode, so that the current is determined only by how fast the substrate is transported to the surface. The kinetic contribution to the current on polymer modified electrode is given by:

$$i_k = nFAKC\Gamma \qquad 13$$

Where K is the rate constant and Γ is the surface coverage of the electroactive electrode. The surface coverage can be evaluated from the equation Γ =Q/nFA

In the case of thin films of supported catalyst the Koutecky–Levich plots can be expressed, assuming that reaction in oxygen species is first order and that the electron transfer is the

rate-determining step. A plot of $1/ i_L$ Vs $\omega^{-1/2}$ (Koutecky-levich) plot should yield a straight line whose slope is related to the number of electron transferred (n) and whose intercept corresponds to the reciprocal kinetic current ($1 /i_K$). A Koutecky-levich plot allows one to separate the effects of rate limitation within the film from those of convective diffusion outside. This plot is a convenient means for extrapolating behavior to infinite ω, and it yields $1/i_K$ as intercept. The power of this approach in dealing with modified electrode lies in its generality. The treatment does not require any assumption about the identity of the rate limiting processes within the film. Several different types of activity can affect the rate at which A is converted to B. Species A must arrive at the film-solution boundary by convective diffusion, or it might enter the structure by rate limited partitioning, diffusion to the electrode surface or to a redox site within the film; there might be a rate limitation in the transfer of electrons at the electrode surface or at the redox site; and there might be a need for electrons to distribute themselves among redox sites throughout the structure. Any of these processes might be rate controlling for the overall conversion. In real systems, one also has to recognize the possibility of pores or pinholes in the film through which A can diffuse to the electrode.[46]

A more general analysis involves separating contribution of electron transfer from other limiting activity inside the film. Therefore the Koutecky-Levich equation ($\frac{1}{i_{obs}} = \frac{1}{i_l} + \frac{1}{i_k}$) eq.11can be re written as :

$$\frac{1}{i_l} = \frac{1}{i_{ldiff}} + \frac{1}{i^0}\exp^{\frac{\eta}{b}} \qquad 14$$

The equation assumes the electron transfer step is the rate determining and occur at large overvoltage.

Where i_{ldiff} limiting current density for the diffusion in the bulk electrolyte

i_l limiting current density resulting from a mixed control inside film other than electron transfer at the electrode (Since this current is independent of ω and E, it is not possible to separate their contribution)

η the over voltage (E^0 – E) Where E is the electrode potential, and E^o is the thermodynamic potential calculated from the ($E^0 = \frac{\Delta G^0}{nFG}$)[45]

The intercept at the origin (ω→ ∞) of Koutecky-levich plot (1/ i vs $\omega^{-1/2}$) gives the inverse of the kinetic current, as a function of the overvoltage, i.e.:

$$\frac{1}{i_k} = \frac{1}{i_l} + \frac{1}{i^0}\exp^{\frac{\eta}{b}} \qquad 15$$

Thus these equation shows that for high overvoltage (|η|→ ∞) the quantity 1/ i_K tends towards 1/ i_l, so that one can obtain the limiting current density i_l by extrapolating eq.16 at high η.This allowed as to transform the above eq. as follow

$$\eta = -b\left[\ln\left|\frac{i_k}{i_l _ i_k}\right| + \ln\frac{i_l}{i^0}\right] \qquad 16$$

Plotting $1/i_k$ as a function of electrode potential E, allowed as determining limiting current (i.e. resulting from a mixed control inside the polymer). Knowing i_l it is possible to plot $\ln\frac{i_k}{i_l _ i_k}$ vs the over potential η gives a straight line with a slope 1/ b and an intercept at the origin [ln (i_l / i_o)].From this results Tafel slope (b) and i_o can be calculated. [47-48]

4. Experimental

4.1 Objectives:

- To examine the electrochemical behavior and the electrocatalytic activity of poly(o-phnylenediamine) (PoPDA), and poly(3,4-ethylenedioxy thiophene) (PEDOT) using cyclic voltammetry and rotating disk voltammetry.
- To determine the kinetic parameters for oxygen reduction reaction on of poly(o-phenylenediamine) (PoPDA), and poly(3,4-ethylenedioxy thiophene) (PEDOT) multiwall carbon nanotube (MWCNT)modified glassy carbon electrode.

4. 2. Apparatus

Electrochemical measurements were performed using Epsilon Electrochemical Workstation with a conventional three electrode system. Glassy carbon with 3 mm in diameter was used as working electrode, platinum wire as counter electrode. All the cell potentials were measured with respect to Ag/AgCl/[KCl (3M)] reference electrode. Hydrodynamic voltammetric studies for oxygen reduction reaction were performed using a rotating disk assembly. An electronic digital balance was used to measure the weights of solid chemicals during solution preparation.

4.3. Chemicals and Reagents

0.05μm Al_2O_3 was used for polishing the electrode surface. Distilled water, multiwalled carbon nanotubes, analytical grade sodium sulphate, sulphuric acid and nitric acid were used. The supporting electrolyte used for electrochemical experiment was 0.2 M Na_2SO_4(pH = 1.0).The aqueous solutions were prepared using distilled water. The monomers used in the electrosynthesis study were o-Phenylenediamine(oPDA) and 3,4- ethylenedioxy thiophene(EDOT).

4.4. Preparation of the Modified Electrodes

About 50 mg of Multi-walled carbon nanotubes were purified by refluxing in a 24cm^3 mixture of concentrated sulphuric and nitric acids (1:1, v/v) for 2 h at 55 ^{0}C and then for 3 h at 80 ^{0}C, respectively. Afterwards, the nanotubes were washed with deionised water by centrifugation repeating it for several times until the filtrate became neutral. Finally, the MWCNTs were dried under vacuum for 15 h.[49] A homogenous dispersion of MWCNT after 30 munite sonication were casted to the working electrodes which was mechanically polished with alumina powder (Al_2O_3, 0.05μm) up to a mirror finish. Then the electrodes were cycled in 0.2M Na_2SO_4 in a potential range from -0.8V to +0.8V at a sweep rate 50mV/s until a stable voltammogram was obtained.

The electropolymerization was conducted in a three electrode cell with glassy carbon electrode and MWCNT modified glassy carbon electrode as the working electrode, Ag/AgCl as the reference electrode, and platinum wire as the counter electrode. The concentration of the monomers used were 50 mM o- phenylenediamine (oPDA)in 0.2 M Na_2SO_4(pH = 1.0), and 0.01 M 3,4-ethylenedioxy thiophene (EDOT) in 0.1 M tetrabutyleammonium tetrafluoroborate(TBATFB) in acetonitrile (AcN).

5. Results and Discussion

5.1. Electrochemical Polymerization

5.1.1. Electrochemical Polymerization of oPDA

The electropolymerization of oPDA was carried out from a solution containing 50 mM of the monomer and 0.2 M Na_2SO_4 at pH = 1.0 by electropolymerization at the potential between -0.8 and +0.8V at 50mV/s versus Ag/AgCl. A thin film made with 8 deposition cycles was used in all experiments.

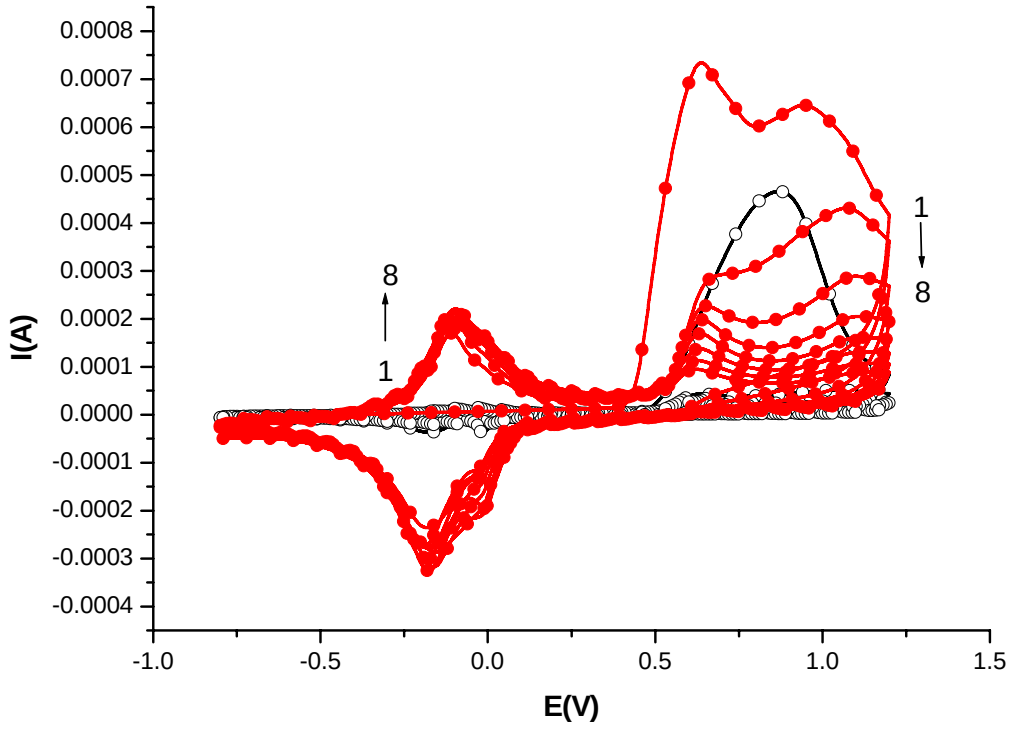


Figure 8. Cyclic voltammogram for the electropolymeriztion of oPDA (○) at glassy carbon electrode and (●) at multi-wall carbon nanotube modified glassy carbon electrode at a scan rate of 50 mV.

A comparison of the cyclic voltametric growth profile of PoPDA at GC and GC/MWCNT (Figure 8) shows that the monomer is easily oxidized at GC/MWCNT electrode than the bare

GC electrode. The peak current for monomer at the GC/MWCNT oxidation is 1.56 times higher than the one at GC. At both electrodes the oxidation peaks begins to appear during first cathodic sweep at more anodic potentials. In subsequent scans, the oxidation peak current were progressively decreased while new peak appeared at less positive potentials indicting the growth of thin film at the electrode.

5.1.2. Electrochemical Polymerization of EDOT

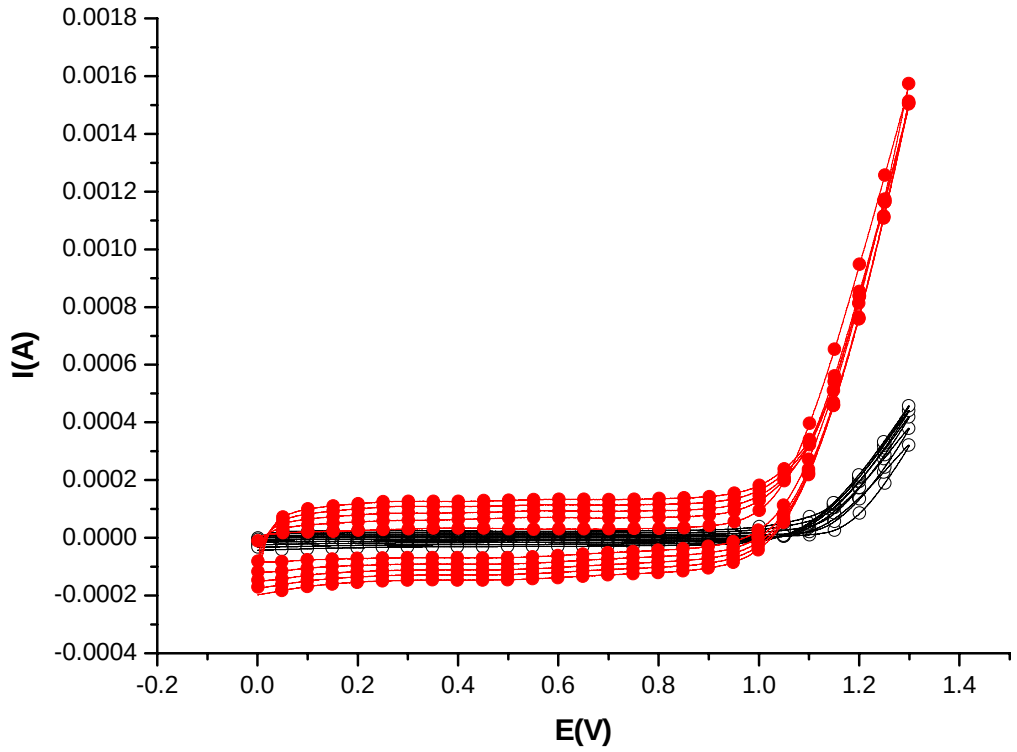


Figure 9.Cyclic voltammogram for the electropolymeriztion of EDOT(○)at GC and (●) at GC/MWCNT at a scan rate of 50 mV/s, in 0.1M tetrabutylammonium tetrafluoroborate in acetonitrle.

The electropolymerization of EDOT was carried out from the electrolyte solution containing 0.01M monomer in 0.1M tetrabutylammonium tetrafluoroborate in acetonitrle (TBATFB/AcN) solution by cycling the potential between - 0.002 and 1.3V at 50 mV/s. A

thin film made with 5 deposition cycles was used in all experiments. A comparison of the cyclic voltametric growth profile of EDOT at GC and GC/MWCNT (Figure 9) shows the monomer is easily oxidized at GC/MWCNT than at GC.

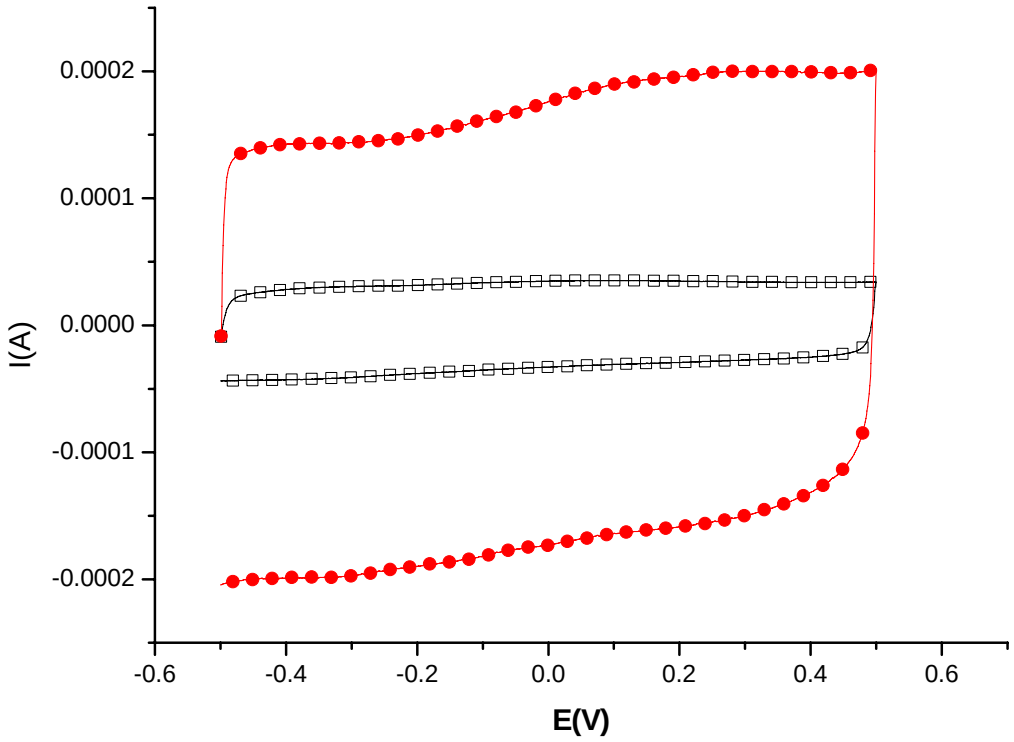


Figure 10. Cyclic voltammogram of monomer free PEDOT (□) at GC (●) at GC/MWCNT at a scan rate of 50 mV/s.

Cyclic voltammograms of the polymer film at GC and GC/MWCNT in monomer free 0.2 M Na_2SO_4 (pH = 1.0) is shown in Figure 10. For the same number of cycles during the electropolymerization thicker film is produced at GC/MWCNT than at GC.

5.2. Cyclic Voltammetric Investigation of the Electrocatalytic Reduction of Oxygen

5.2.1. Electrocatalytic Reduction of Oxygen at GC/MWCNT/PoPDA

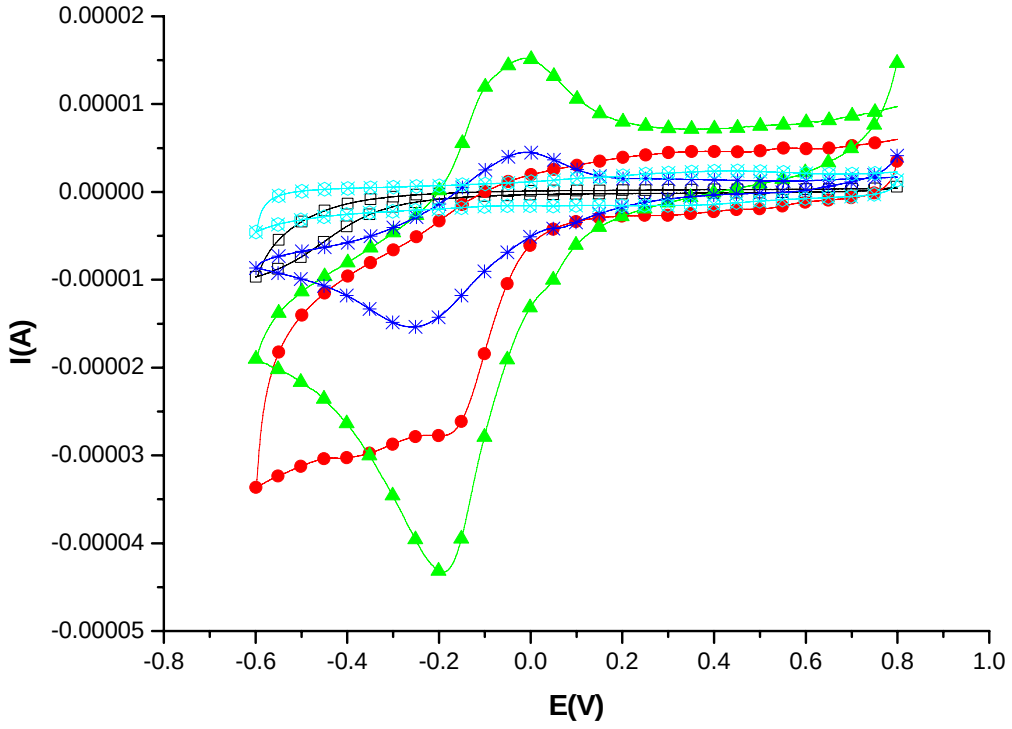


Figure 11. Cyclic voltammograms for the reduction of oxygen in oxygen saturated 0.2 M Na_2SO_4 (PH = 1.0) solution at (□) GC, (✳) GC/PoPDA,(●) GC/MWCNT, (▲)GC/MWCNT/PoPDA and (⊠) in argon saturated at GC/ MWCNT at 20 mV/s.

The electrochemical reduction of oxygen has been studied by cyclic voltammetry at GC, GC/MWCNT, GC/POPDA and GC/MWCNT/POPDA modified electrodes and voltammograms is shown in Figure 11. At GC electrode the cyclic voltammogram shows an ill defined reduction peak at a potential greater than -0.59V, The oxygen reduction peak were significantly shifted to less negative potential at the modified electrodes and were observed at about -0.269 V, -0.206V and at -0.189 V at GC/POPDA, GC/MWCNT and GC/MWCNT/POPDA modified electrodes, respectively. The cathodic peak currents have

also increased at the modified electrodes. For instance, the peak current at GC/MWCNT/POPDA modified electrode is found to be about 2.8 times higher than that of the GC/POPDA modified electrode.

5.2.2. Electrocatalytic Reduction of Oxygen at GC/MWCNT/PEDOT

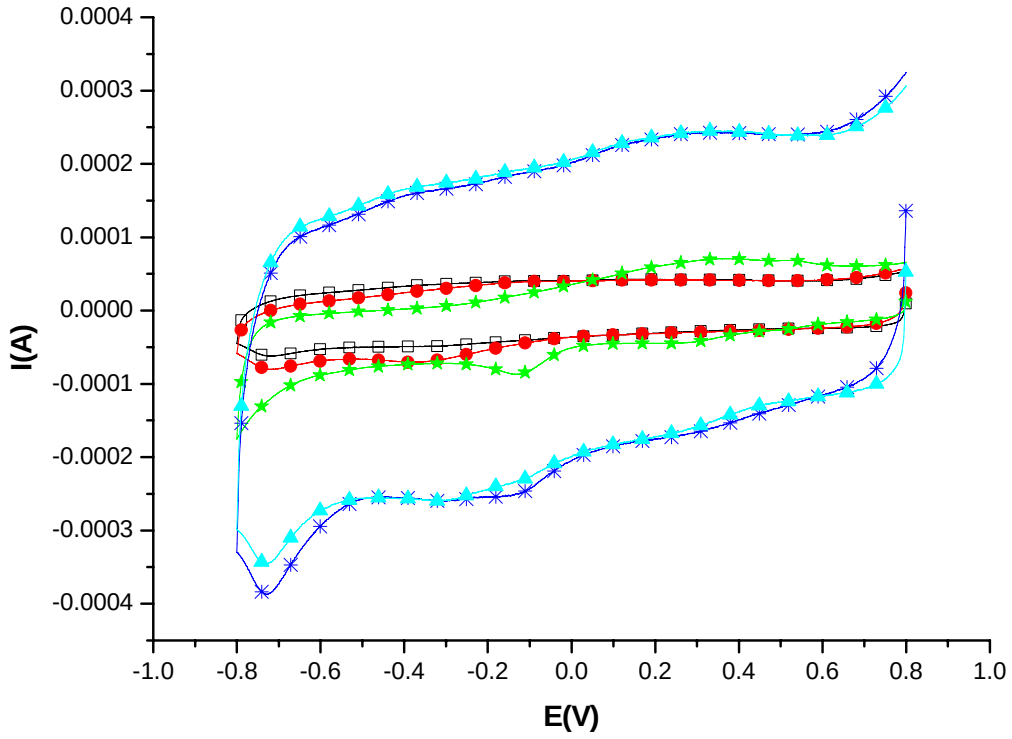


Figure 12. Cyclic voltammograms for the reduction of oxygen in Ar saturated 0.2 M Na_2So_4 at (□) GC/PEDOT,(▲) GC/MWCNT/PEDOT and in oxygen saturated 0.2M Na_2SO_4 (PH= 1.0) solution at (●) GC/PEDOT, (★) GC/MWCNT, (✳) GC/MWCNT/PEDOT at 20 mV/s.

The electrochemical reduction oxygen has also been investigated by cyclic voltammetry at GC/PEDOT and GC/MWCNT/PEDOT modified electrodes and compared with the bare electrode. As can been seen from Figure 12 no significant electrocatalytic behavior for oxygen reduction is observed at both GC/PEDOT and GC/MWCNT/PEDOT modified electrodes.

5.3. Rotating Disk Voltammetric Investigation of the Electrocatatalytic Reduction Oxygen

5.3.1. Oxygen Reduction at MWCNT Modified Glassy Carbon Electrode

The electrocatalytic reduction of oxygen at GC/MWCNT investigated using rotating disk electrode at different rotation speed. A voltammogram is shown in Figure 13.

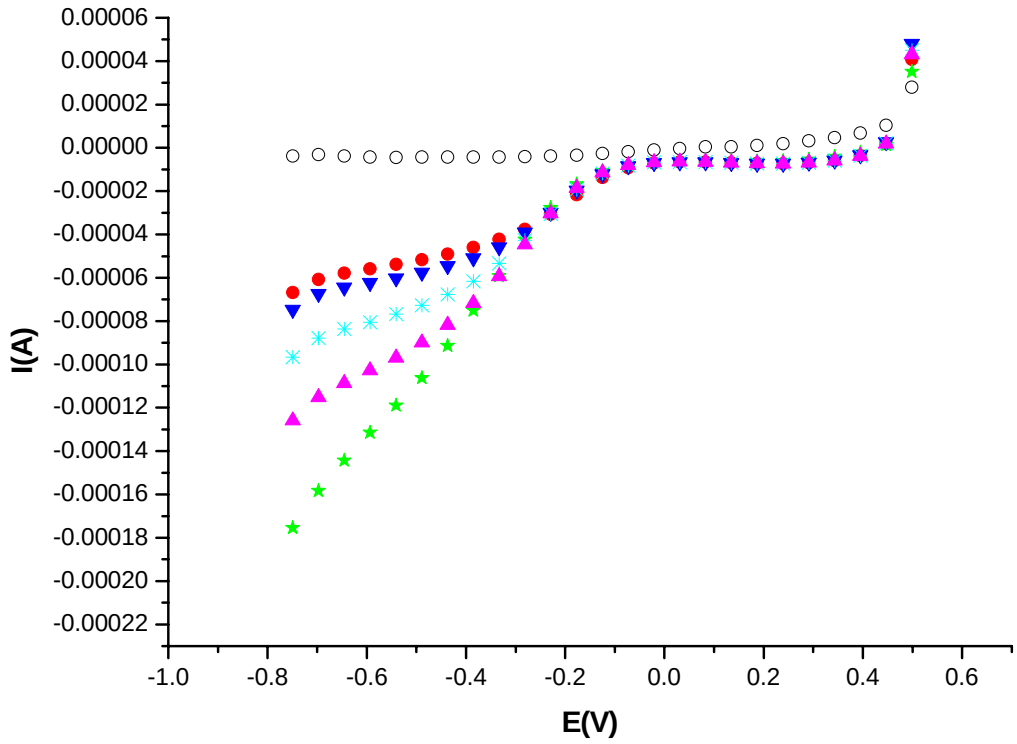


Figure 13. Rotating disk voltammogram for the reduction of oxygen at GC/MWCNT rotating disk electrode at (○) 100 rpm (Ar saturated) and (●) 100, (▼) 200, (✳) 400, (▲) 800 and (★) 1600 (rpm) in O_2 saturated 0.2M Na_2SO_4 at PH = 1.0, 10mV/s.

The oxygen reduction reactions are a complex combination of charge transfer and mass transport processes.[50] A charge-transfer kinetics control with rotation rate-independent current is observed in the range of -0.200-0.60 Vs Ag/AgCl; at more cathodic potentials, mixed control became significant without arriving to a well-defined mass transport-limited current as a function of the rotation rate. It was considered that increases in the limiting

current on high performance electrocatalysts are associated with the increase of molecular oxygen diffusion in the boundary layer thickness through the electrode surface. The reduction reaction is fast enough at high cathodic over potentials, associated in almost all the cases to a flat limiting plateau. An explanation for the well defined current plateau could be the existence of a distribution of electrocatalytic sites on the electrode surface. The current of oxygen reduction increase at a given potential with the increase of rotation rate, this indicates clearly that the reduction of oxygen is diffusion controlled. [50]

A Levich plot (I_d vs $\omega^{1/2}$) for oxygen reduction reaction at GC/MWCNT electrode in an O_2 saturated 0.2M Na_2SO_4 solution is shown in Figure 14.

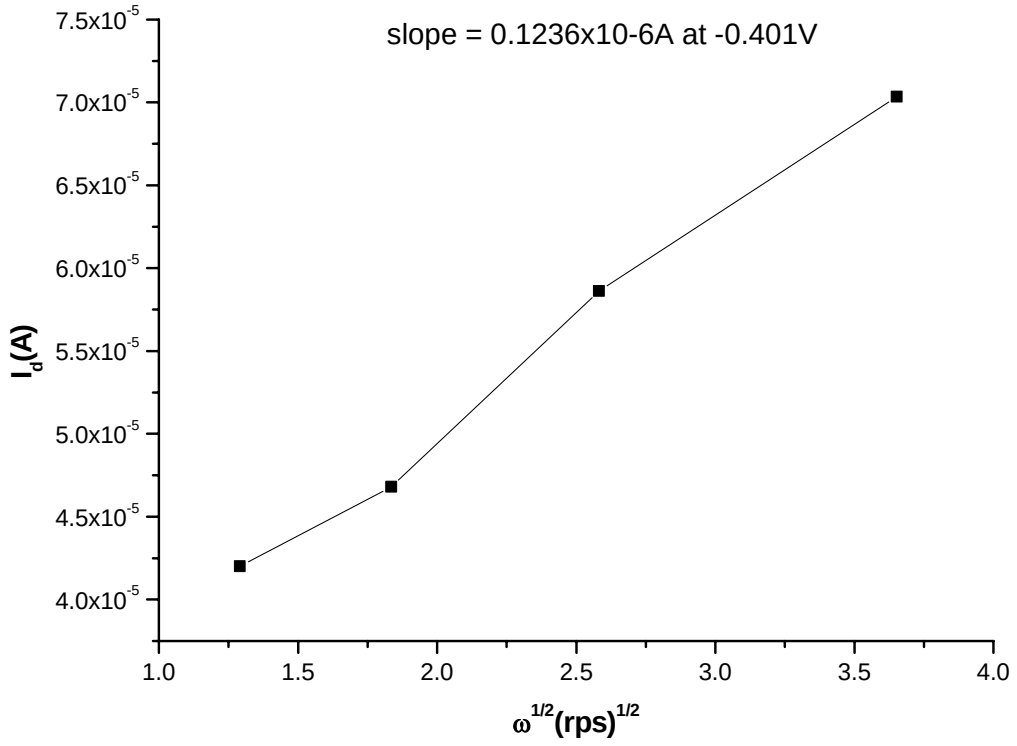


Figure 14. Levich plots for the reduction of oxygen at MWCNT modified glassy carbon electrode in (O_2 saturated 0.2M Na_2SO_4,10mV/s).

The values used for calculation of theoretical Levich plots were: D = $2.1x10^{-5}$ cm^2 s^{-1} for the diffusion coefficient of molecular oxygen,ν = $1.075x10^{-2}$ cm^2 s^{-1} for the kinematic viscosity of oxygen [32], the faraday constant, F = 96485 C/mol, area of the disk electrode, A=

$0.0707cm^2$ geometric surface area and concentration of dissolved oxygen, $C=1.03x10^{-6}moldm^{-3}$.

Figure 15 shows Koutecky-levich plots I_d^{-1} vs $\omega^{-1/2}$ (with data taken from Figure 14). Straight line are obtained the slope (0.0302 μA $(rps)^{-1/2}$) of which yielding n = 4.39 agrees reasonably well with the theoretical value (0.035302μA $(rps)^{-1/2}$) for four electrons process. Therefore, the reduction of oxygen is a direct reduction path way, (i.e the reduction of O_2 directly to H_2O) through four electron transfer.

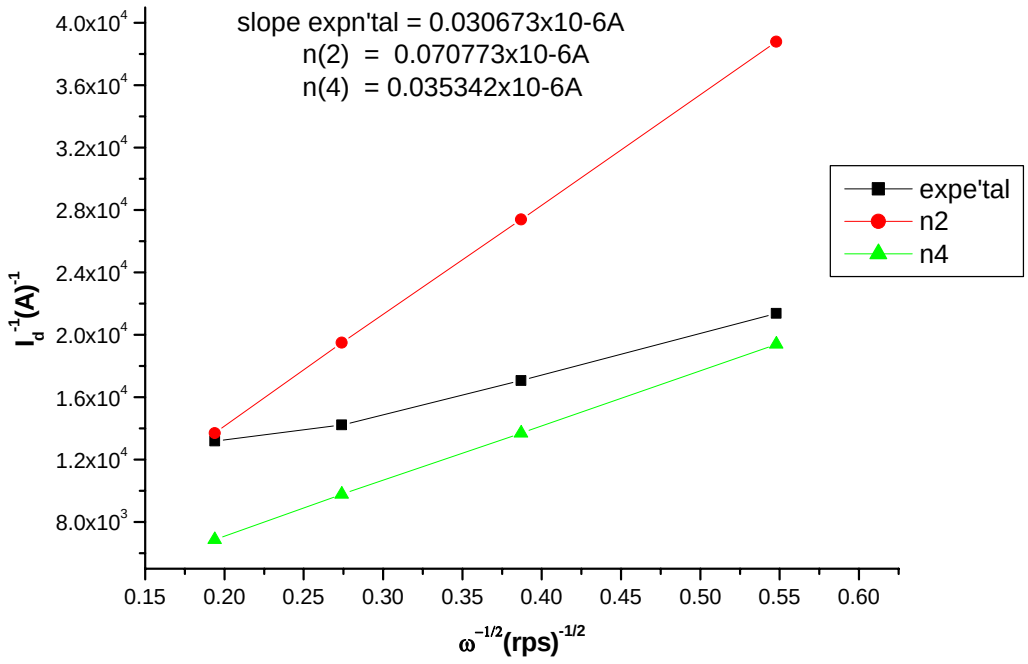


Figure 15. Koutecky- levich plot I_d^{-1} vs $\omega^{-1/2}$ for the reduction of oxygen at GC/MWCNT rotating disk electrode (O_2 saturated 0.2M Na_2SO_4, 10mV/s) for theoretical (2es and 4es) and experimental result.

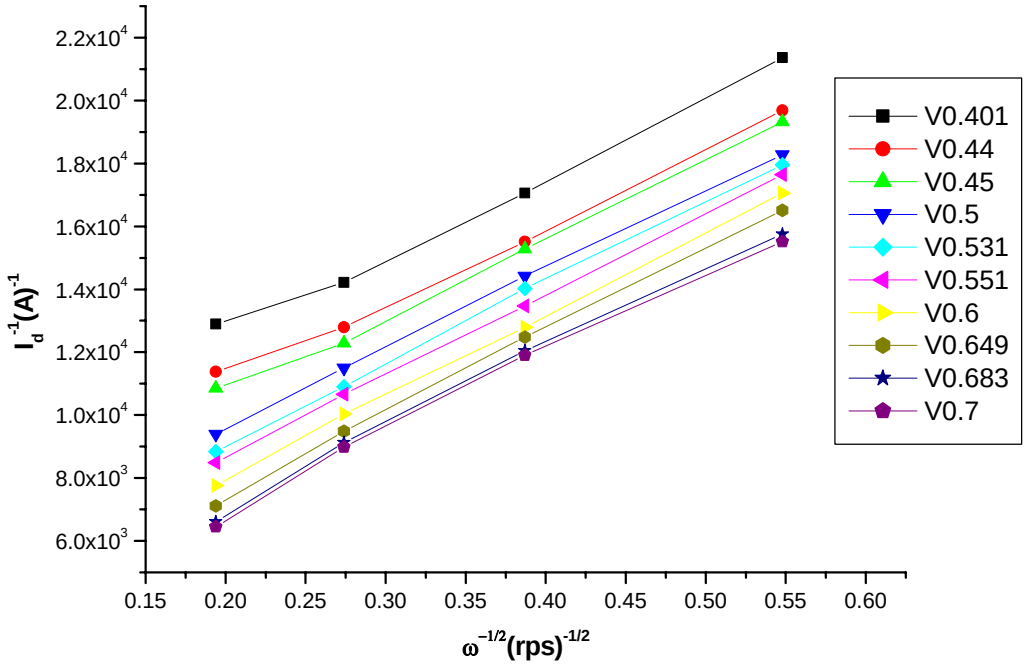


Figure 16. Koutecky-levich plot I_d^{-1} vs $\omega^{-1/2}$ for the reduction of oxygen at GC/MWCNT rotating disk electrode (O_2 saturated 0.2M Na_2SO_4, 10mV/s) at different potentials.

Figure 16 Koutecky-levich plot I_d^{-1} vs $\omega^{-1/2}$ at different electrode potentials. Straight line are obtained indicating a constant number of electrons involved in the reduction reaction [50] and the intercept at infinite rotation speed or at high potential gives $1/i_k$. Then plotting $1/i_k$ as a function of the electrode potential E (Figure 17) allowed as to determine the limiting current densityi_l.

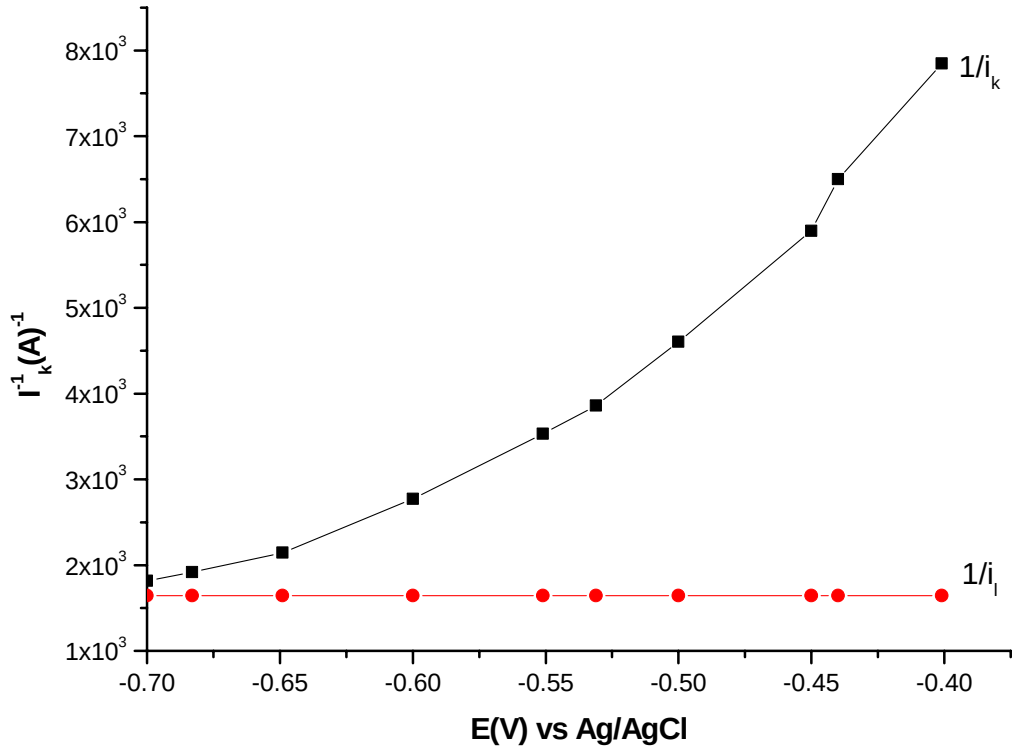


Figure 17. Plot of $1/i_k$ vs the electrode potential for the reduction of oxygen at GC/MWCNT rotating disk electrode(O_2 saturated 0.2M Na_2SO_4,10mV/s.)

The value of $1/i_l$ obtained from Figure 17 at GC/MWCNT is $1644.3A^{-1}$ and i_l found to be $6.08x10^{-4}$A. Knowing i_l it is possible to plot E vs ln $[i_k/(i_l-i_k)]$ which also gives straight line (Figure18) from the slope of which the Tafle slope b is obtained, and from the intercept of which at the equilibrium potential and the exchange current density i^o can be evaluated.

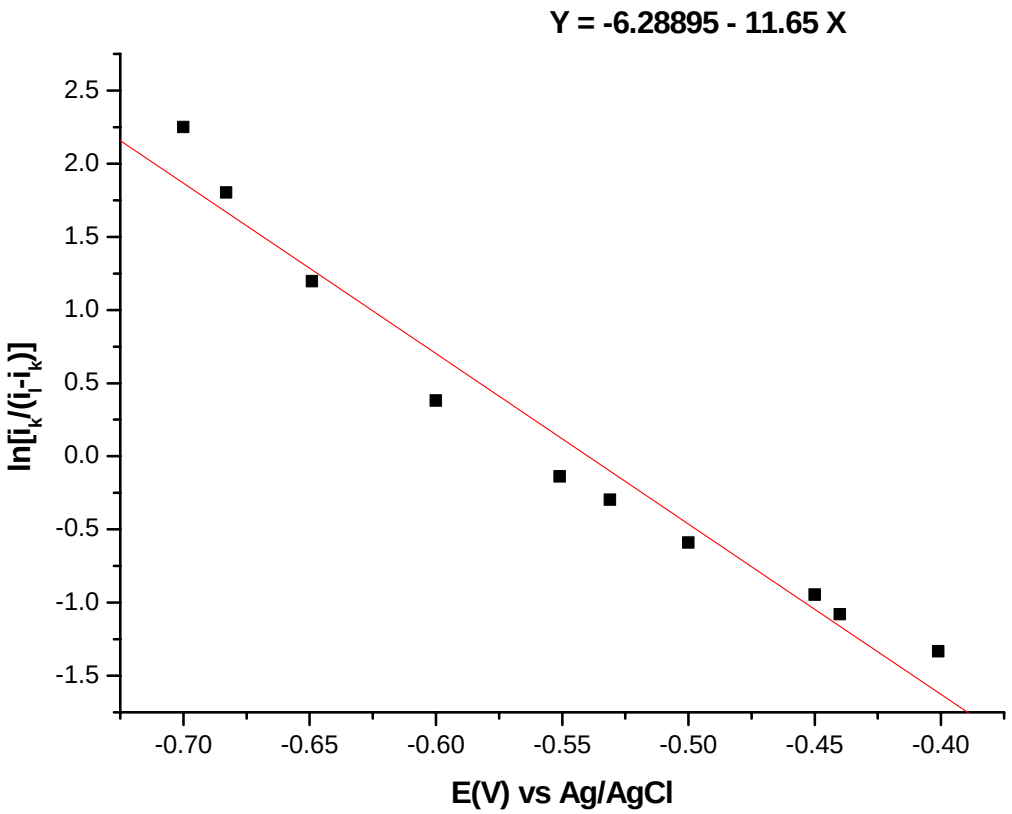


Figure 18. Plot ln[i_k/ ($i_l - i_k$)] vs the electrode potential E for the reduction of oxygen at GC/MWCNT rotating disk electrode (O_2 saturated 0.2M Na_2SO_4, 10mV/s).

Figure 18 plot ln [i_k / ($i_l - i_k$)] vs E shows straight line with a slope 1/ b (11.65dec / V) and an intercept - ln (i_l / i^o) (-6.29). From these results a Tafel slope 85.84mV / dec and an exchange current of 1.1288 x 10^{-6} were calculated. The limiting current (i_l) is much higher (by a factor of 506.7times)to that of the exchange current density.

5.3.2. Oxygen Reduction at MWCNT/PoPDA Modified Glassy Carbon Electrode

The electrocatalytic reduction of oxygen at GC/MWCNT/PoPDA was investigated using a rotating disk electrode (RDE) at different rotation speed. Typical voltammogram is shown in Figure 19.

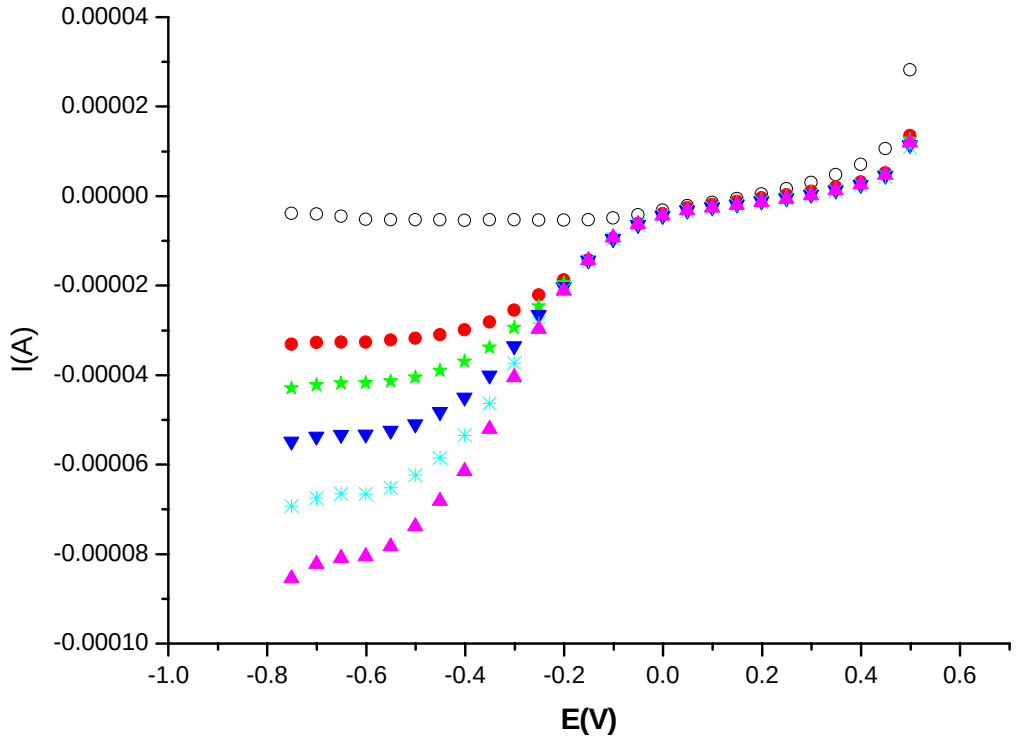


Figure 19. Rotating disk voltammogram for the reduction of oxygen at GC/MWCNT/PoPDA rotating disk electrode at (○)100 rpm (Ar saturated) and (●) 100, (★) 200, (▼) 400, (✳) 800 and (▲) 1600 (rpm) in O_2 saturated 0.2M Na_2SO_4 at PH1.0, 10mV/s.

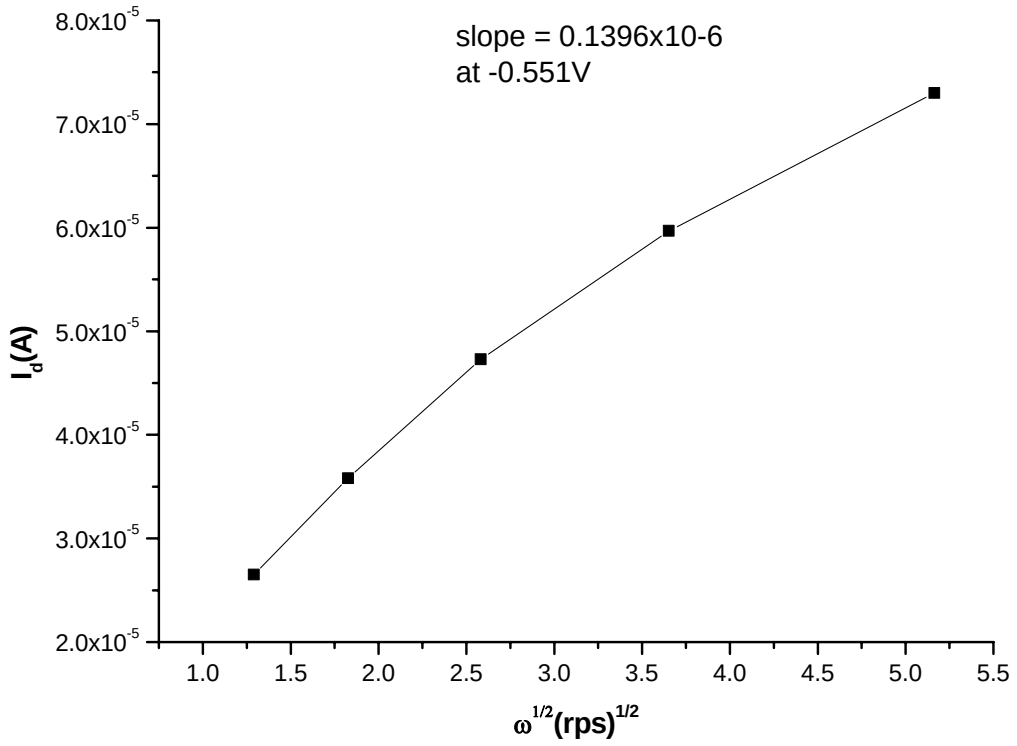


Figure 20. Levich for the reduction of oxygen at GC/MWCNT/PoPDA rotating disk electrode (O_2 saturated 0.2M Na_2SO_4, 10mV/s).

Figure 20 and 21 the Levich and Koutecky – Levich plots for ORR at GC/MWNT/PoDA respectively. From Koutecky-levich plots I_d^{-1} vs $\omega^{-1/2}$ (with data taken from Figure 19) straight line are obtained the slope (0.04137 μA $(rps)^{-1/2}$) of which yielding n = 3.18 which is approximately equal to the theoretical value (0.035302μA $(rps)^{-1/2}$) for four electrons process. Therefore the reduction of oxygen is a direct reduction path way, (i.e the reduction of O_2 directly to H_2O) through four electron transfer.

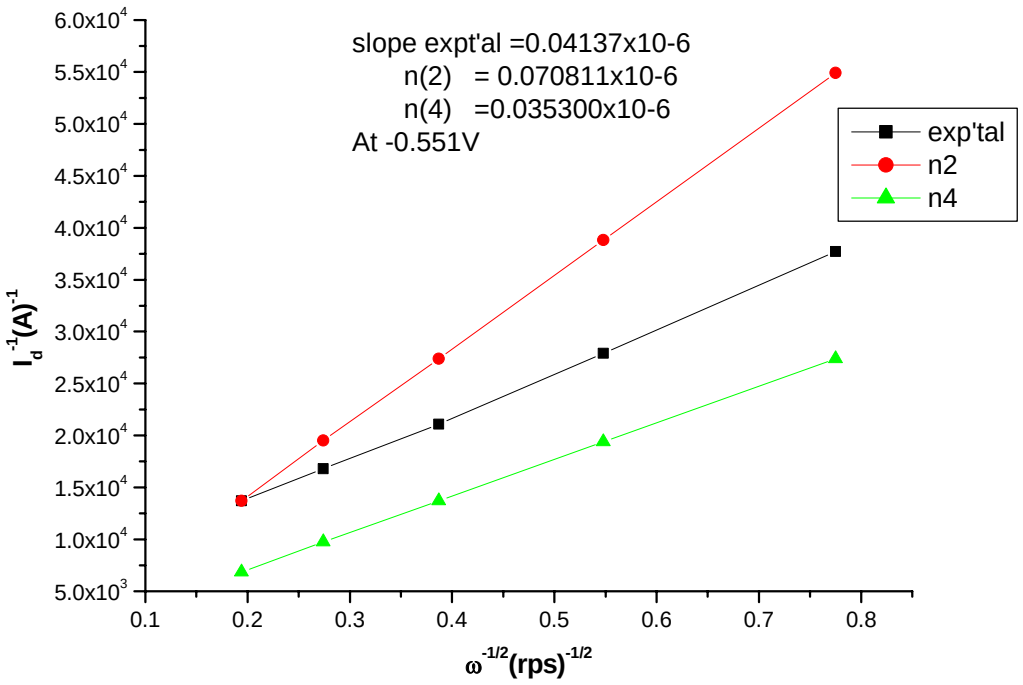


Figure 21. Koutecky-levich plot I_d^{-1} vs $\omega^{-1/2}$ for the reduction of oxygen at GC/MWCNT/PoPDA rotating disk electrode (O_2 saturated 0.2M Na_2SO_4, 10mV/s) for theoretical (2es and 4es) and experimental result.

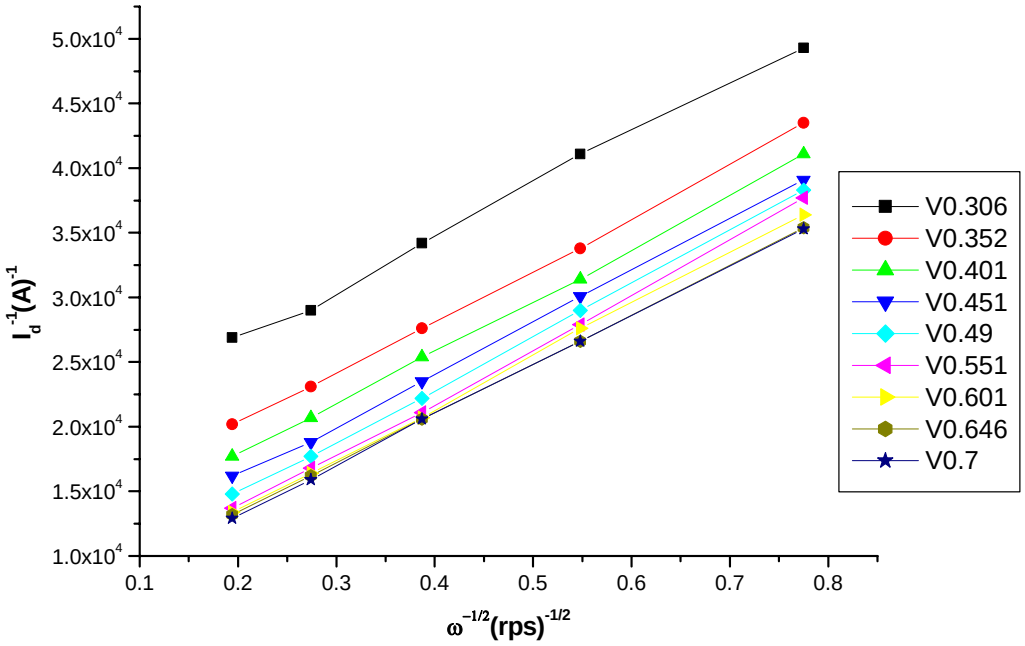


Figure 22. Koutecky- levich plot I_d^{-1} vs $\omega^{-1/2}$ for the reduction of oxygen at GC/MWCNT/PoPDA rotating disk electrode (O_2 saturated 0.2M Na_2SO_4, 10mV/s) at different potentials.

Figure 22 Koutecky- levich plot I_d^{-1} vs $\omega^{-1/2}$ for the reduction of oxygen at GC/MWCNT/PoPDA rotating disk electrode. At all the rotation speeds, as expected, a series of essentially parallel straight lines over a broad potential range (-0.306 – 0.7) is illustrated. Parallelism of the straight lines indicates that the number of electrons transferred per O_2 molecule and the active surface area for the reaction do not change significantly within the potential range studied. And the intercept at infinite rotation speed or at high potential gives $1/i_k$. Then plotting $1/i_k$ as a function of the electrode potential E (Figure 23) allowed as to determine the limiting current density i_l.

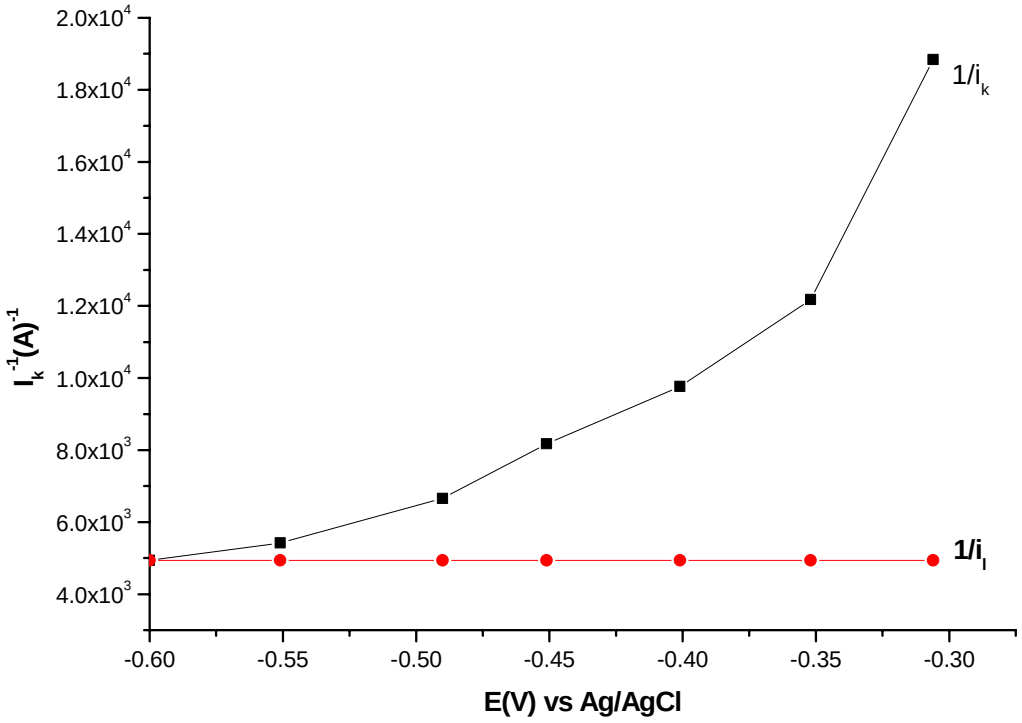


Figure 23. Plot of $1/i_k$ vs the electrode potential for the reduction of oxygen at GC/MWCNT/PoPDA rotating disk electrode (O_2 saturated 0.2M Na_2SO_4,10mV).

The value of $1/i_l$ obtained from Figure 23 for GC/MWCNT/PoPDA is $4934A^{-1}$ and i_l found to be $2.067x10^{-4}$A. Knowing i_l it is possible to plot E vs ln $[i_k/(i_l-i_k)]$ which also gives straight line (Figure 24) from the slope of which the Tafle slope b is obtained, and from the intercept of which at the equilibrium potential, the exchange current density i^o can be evaluated.

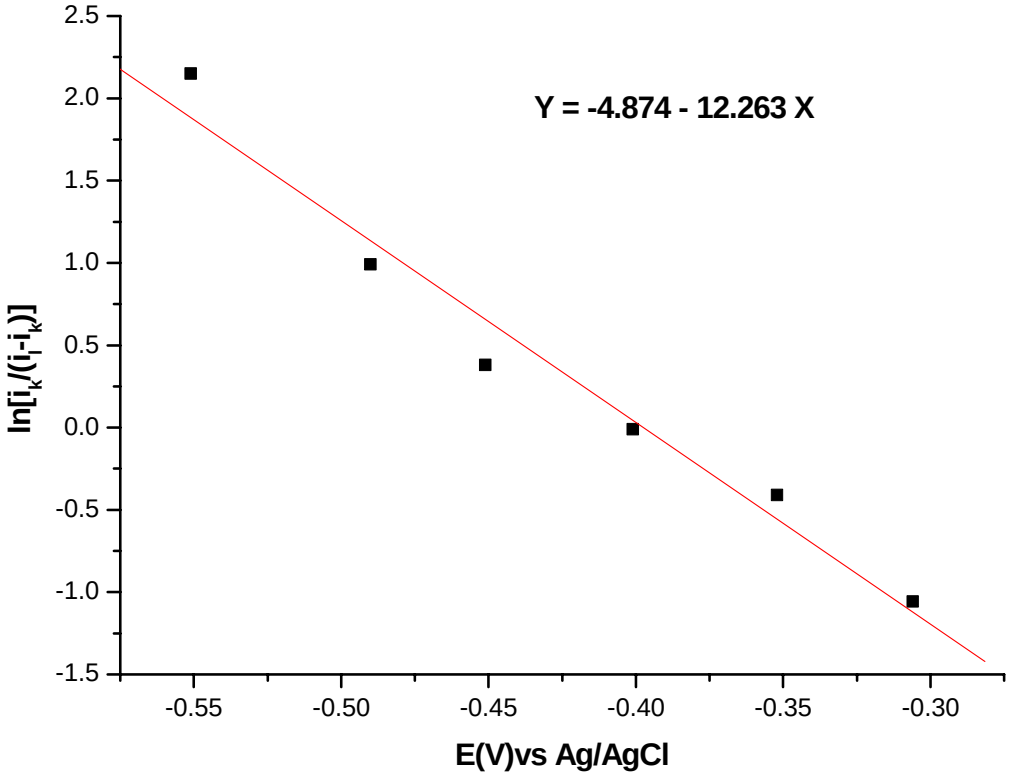


Figure 24. Plot ln[i_k/ (i_l – i_k)] vs the electrode potential E for the reduction of oxygen on GC/MWCNT/PoPDA rotating disk electrode (O_2 saturated 0.2M Na_2SO_4, 10mV/s).

Figure 24 plot ln [i_k /(i_l – i_k)] vs E shows a straight line with a slope 1/ b (12.263dec / V) and an intercept - ln (i_l / i^o) (-4.874). From these results a Tafel slope 81.5mV / dec and an exchange current of 1.574x 10^{-6} were calculated. The limiting current (i_l) is much higher by a factor of 279.5 times that of the exchange current i^o. This confirms that the electron transfer step is rate determining.

The kinetic parameters for oxygen reduction at PoPDA modified glassy carbon electrode was taken from the previous work, and the compression of the kinetic parameters at GC modified with PoPDA, MWCNT and MWCNT/PoPDA composite electrode was given by;

GC modified with	Limiting current i_l	Tafel slope (b/ mV/dec)	Exchange current i^o
PoPDA	2.15×10^{-4}	65.75	1.33×10^{-7}
MWCNT	6.08x10-4	85.58	1.2x10-6
MWCNT/PoPDA	1.8×10^{-4}	81.548	1.574×10^{-6}

Table1 Kinetic parameter for oxygen reduction reaction at PoPDA, MWCNT and MWCNT/PoPDA modified glassy carbon electrodes.

Oxygen reduction activity was measured in terms of current density at a potential where the oxygen reduction kinetics is more favourable and/or potential at which maximum reduction current occurs. But in commercial point of view, one requires a catalyst, which has the ability to reduce oxygen at higher potentials with high current densities. Based on this criteria MWCNT/PoPDA modified GC electrode with the highest exchange current will be the best electrocatalytst for oxygen reduction reaction. The RDV experimental result have shows that four electrons are involved in the charge transfer process and this means that molecular oxygen is directly converted to water.

Previously in the literature GC/MWCNT/PoPDA composite for oxygen reduction reaction were studded. But the modification method of the MWCNT was different the one in this study(the nanotube is subjected to chemical oxidation treatment with a mixture of concentric nitric and sulphuric acid in a ratio of 1:3 respectively). And the number of electrons transferred in oxygen reduction calculated from the Koutecky-Levichplots was found to be 1.5 and 1.7 for GC/MWCNT and MWCNT/PoPDA respectively.[51] This indicates that as the modification of MWCNT is changed the reaction path ways for oxygen reduction is also changed.

6. Conclusion

Electrochemical behaviour and electrocatalytic reduction of oxygen has been studied on PoPDA, and PEDOT muti-wall carbon nano-tube (MWCNT) composite modified glassy carbon electrode by cyclic voltammetric and rotating disk voltammetric techniques. PoPDA multiwall carbon nanotube composite electrode shows enhanced electrocatalytic behaviour for the reduction of oxygen but MWCNT/PEDOT modified electrode did not show. The kinetic parameters n i^0 i_l and b were evaluated at GC/MWCNT and GC/MWCNT/PoPDA composite electrode.

In this study it was showed that the presence of a specific chemical interaction between the acid treated (COOH group of) MWCNT and to that of (NH of) PoPDA resulting in a very good enhancement in the electrochemical property of the polymer. This enhancement indicts that the usefulness of the material in the electrochemical sensors. The readily soluble nature of the PoPDA/MWCNT composite in aqueous solution may be help full in realizing several applications of such polymers including the construction of electronic devices and as coating for corrosion protection.

7. References

[1]. J. Lipkowski and P.N. Ross, Electrocatalysis, Wiley-VCH, New York, 1998.

[2]. J. X. Wang, N. M. Markovic, R. R. Adzic, J. Phys. Chem. B, 108, 4127, 2004.

[3]. A.K. Shukla and R.K. Raman. Annu. Rev. Mater. Res. 33, 155–68, 2003.

[4]. H.Meng, P. K. Shen, Electrochemistry Communications, 8, 588–594, 2006.

[5]. L. Pauling, Nature ,203, 182, 1964.

[6]. H. S. Wroblowa, Y. C. Pan and G. Razumney, J. Electroanal. Chem., 69, 195, 1976.

[7]. A. Damjanovic, M. A. Gensaw and J. O'M. Bockries, J. Chem. Phys., 45, 4057, 1966.

[8]. A.J. Bard, L.R. Faulkner, Electrochemical Methods: Fundamentals and Applications, 2nd ed., John Wiley and Sons, New York, 2000.

[9]. C. Song, Y. Tang, J. Zhang, J. Zhang, H. Wang, and J. Shen, Electrochim. Acta, 52, 2552–61, 2007.

[10]. A. Damjanovic. J. Electroanal. Chem., 355, 57–77, 1993.

[11] A. Damjanovic, J. Electrochem. Soc. 138, 2315, 1991.

[12]. F. King, M. J. Quinn and C. D. J. Electroanal. Chem., 45, 385, 1995.

[13]. C. Charles, and A. L. Juliard, J. Electroanal. Chem., 9, 390, 1965.

[14]. P. Gouerec, M. Savy and J. Riga, Electrochim. Acta, 43, 743, 1998.

[15]. K. Sawai and N. Suzuki, J. Electrochem. Soc., 151, 682, 2004.

[16]. D. P.Catalan, E. Morales, M. Smit and J. L. Acosta1 J. New Mat. Electrochem. Systems 12, 115-118, 2009.

[17]. E. Deiss, F. Holzer and O. Haas, Electrochim. Acta, 47, 3995, 2002.

[18]. M. Winter and R. J. Brodd, Chem. Rev., 104, 4245, 2004.

[19]. http://www.eere.energy.gov/industry/imf/pdfs/lanl_chlor_alkali.pdf, (2010, 5, 20, 9:32)

[20]. M. Daenen, R.D. de Fouw, B. Hamers , P.G.A. Janssen, K. Schouteden and M.A.J. Veld , The Wondrous World of Carbon Nanotubes, 2003.

[21]. G. Korneva, A Thesis Submitted to the Faculty of Drexel University, 2008.

[22]. K. Balasubramanian and M. Burghard J. of Mate. Chem.,18, 3071, 2008.

[23]. R.N. Goyal, A. Tyagi, N. Bachheti, and S. Bishnoi, Electrochim., Acta, 53, 2802, 2008.

[24]. J. O. M. Bockries and A. K. N. Reddy, Modern Electrochemistry, Plenum Press, New York, 1970.

[25]. J. B. Goodenough and B. L. Hand book of Fuel Cells – Fundamentals, Technology and applications, Electrocatalysis, John Wiley & Sons, 2003.

[26]. A. J. Appleby, J. Electroanal. Chem. 357, 117, 1993.

[27]. M. Maja, C. Orecchia, M. Strano, P. Tosco and M. Vanni, Electrochim. Acta, 46, 423. 2000.

[28]. Q. Xu, S.F. Wang, Microchim. Acta, 151, 47, 2005.

[29]. H. Qi, C. Zhang, Electroanalysis, 17, 832, 2005.

[30]. Y. Zhang, W. Cheng, S. Li, and N. Li, Colloids Surf., 286, 33-38, 2006.

[31]. N. Alexeyeva, and K.Tammeveski, Anal. Chem. Acta, 618, 140-146, 2008.

[32] K. M. Manesh, P. Santhosh, A. I. Gopalan, and K. Lee, Electroanalysis, 18, 1564 – 1571, 2006.

[33]. A. Malinauskas, J. Malinauskiene and A. Ramanavicius, Nanotechnology, 16, 51–62, 2005.

[34]. V.G. Khomenko, V.Z. Barsukov, and A.S. Katashinskii, Electrochim. Acta, 50, 1675, 2005.

[35]. J. Wang, M. Li, Z. Shi, N. Li, and Z. Gu, Anal. Chem., 74, 1993, 2002.

[36]. M. Musameh, J. Wang, A. Merkoci, and Y. Lin, Electochem. Commun., 4, 743, 2002.

[37]. J. Wang, M. Li, Z. Shi, N. Li, and Z. Gu, Electroanalysis, 14, 225, 2002.

[38]. J. Wang, M. Musameh, and Y. Lin, J. Am. Chem. Soc., 125, 2408, 2003.

[39]. Y. D. Zhao, W. D. Zheng, H. Chen, and Q. M. Luo, Talanta, 58, 529, 2002.

[40]. C. H. Yang, and T. C. Wen, J. Electroanal. Chem., 459, 99, 1998.

[41]. G. Wu, L. Li, J. H. Li, B. Q. Xu, Carbon, 43, 2579, 2005.

[42]. K. Ding, Electrochim., Acta, 27, 165-175, 2009.

[43]. R. N. Adams and M. Dekker, Electrochemistry at Solid Electrode, New York, 1969.

[44]. J. Wang, Analytical Electrochemistry, 3rd ed., John Wiley and Sons, New York, 2006.

[45]. E. Yeager, J.O.M. Bockris, B. E. Conway and S. Sarangapani, Comprehnesive Treatise of Electrochemistry, 9, Plenum Press, New York, 1984

[47]. J. Koryta, J. Dvorak, and L. Kavan , Principles of Electrochemistry, 2nd ed., John Willey and Sons, New York, 1987.

[48]. B.C. Kappl, Instrumental Method in Electrochemistry, Harwood Publishing Chichester, England, 2004.

[49]. N. Alexeyeva, J. Kozlova, V. Sammelselg, P. Ritslaid, H. Mandar, and K.

Tammeveski, Applied Surface Science 256, 3040–3046, 2010.

[50]. P. Sotelo-Mazón, R.G. González-Huerta, J. G. Cabañas-Moreno, and O. Solorza-Feria, Int. J. Electrochem. Sci., 2, 523 – 533, 2007.

[51]. P. Gajendran, and R. Saraswathi, J. Phys. Chem., C, 111, 11320-11328, 2007.